Arch Virol (2016) 161:3095–3124
DOI 10.1007/s00705-016-2988-3

ORIGINAL ARTICLE

A polydnaviral genome of *Microplitis bicoloratus* bracovirus and molecular interactions between the host and virus involved in NF-κB signaling

Dong-Shuai Yu[1] · Ya-Bin Chen[1] · Ming Li[1] · Ming-Jun Yang[2] · Yang Yang[1] · Jian-Sheng Hu[1] · Kai-Jun Luo[1]

Received: 15 February 2016 / Accepted: 15 July 2016 / Published online: 13 August 2016

Abstract Polydnaviruses (PDVs) play a critical role in altering host gene expression to induce immunosuppression. However, it remains largely unclear how PDV genes affect host genes. Here, the complete genome sequence of *Microplitis bicoloratus* bracovirus (MbBV), which is known to be an apoptosis inducer, was determined. The MbBV genome consisted of 17 putative double-stranded DNA circles and 179 fragments with a total size of 336,336 bp and contained 116 open reading frames (ORFs). Based on conserved domains, nine gene families were identified, of which the IκB-like viral ankyrin (*vank*) family included 28 members and was one of the largest families. Among the 116 ORFs, 13 MbBV genes were expressed in hemocytes undergoing MbBV-induced apoptosis and further analyzed. Three *vank* genes (*vank86*, *vank92*, *vank101*) were expressed in hemocytes collected from *Spodoptera litura* larvae parasitized by *M. bicoloratus*, in which host NF-κB/IκBs, including *relish*, *dorsal*, and *cactus*, were also persistently expressed. When Spli221 cells were infected with MbBV viral particles, mRNA levels of host and viral NF-κB/IκB genes were persistent and also varied in Spli221 cells undergoing virus-induced pre-apoptosis cell from 1 to 5 hours postinfection. Both were then expressed in a time-dependent expression in virus-induced apoptotic cells. These data show that viral IκB-like transcription does not inhibit host NF-κB/IκB expression, suggesting that transcription of these genes might be regulated by different mechanisms.

Abbreviations

MbBV	*Microplitis bicoloratus* bracovirus
MdBV	*Microplitis demolitor* bracovirus
CcBV	*Cotesia congregata* bracovirus
CsBV	*Cotesia sesamiae* bracovirus
CvBV	*Cotesia vestalis* bracovirus
CiBV	*Chelonus inanitus* bracovirus
PDV	polydnavirus
Vank	viral ankyrin

Introduction

Delivery of viral particles and eggs to the host hemocoel involves the development of immature parasitoid offspring through the stages of eggs, embryos, first-instar, second-instar, and third-instar larvae, which must occur in the absence of the ability of the larva to protect itself against the host cellular immune response. Braconid and ichneumonid wasps that carry polydnaviruses (PDVs) [37] require the immunosuppressive function of a virus to avoid host non-self recognition. The viral family *Polydnaviridae* is divided into two genera, *Bracovirus* and *Ichnovirus*. Bracoviruses (BVs) and ichnoviruses (IVs) have independent origins, but share a similar life style, probably through a

D.-S. Yu, Y.-B. Chen and M. Li are equal contributors.

Electronic supplementary material The online version of this article (doi:10.1007/s00705-016-2988-3) contains supplementary material, which is available to authorized users.

✉ Kai-Jun Luo
kaijun_luo@ynu.edu.cn

[1] Key Laboratory for Animal Genetic Diversity and Evolution of High Education in Yunnan Province, School of Life Sciences, Yunnan University, Kunming 650091, People's Republic of China

[2] Shanghai-MOST Key Laboratory of Health and Disease Genomic, Chinese National Human Genome Center at Shanghai, Shanghai 201203, People's Republic of China

convergent evolutionary process [40]. The proviral form of the viral genome is transmitted vertically in wasps; viral DNA replication only occurs at the pupal-adult stage in ovarian calyx cells in the female wasp [1]. Mature virus particles are stored in the lumen of the calyx and oviduct and are injected along with the egg into the lepidopteran host hemocoel. The viral genome is then integrated into the wasp's host chromosome(s) to transcribe the viral genes to inhibit host immune responses to ensuring proper development of the wasp larva [3, 6, 12, 35–37]. These immunosuppressive processes are controlled mainly by viral genome transcription and its effect on the expression of host genes.

Several BV genomes have been sequenced. The viral genome sizes range from 200 kilobase pairs (kbp) in *Microplitis demolitor* bracovirus (MdBV) to 600 kbp in *Cotesia vestalis* bracovirus (CvBV) in separate circles: 15 circles in MdBV and 35 circles in CvBV. The number of predicted open reading frames (ORFs) varies from 61 in MdBV to 157 in CvBV [8, 40]. Over 20 protein families have been identified from BVs, *Cotesia congregata* bracovirus (CcBV) (total 80 genes in 16 protein families), CvBV (total 91 genes in 17 protein families), *Glyptapanteles indiensis* bracovirus (GiBV) (total 87 genes in 16 protein families), *G. flavicoxis* bracovirus (GfBV) (total 79 genes in 15 protein families), and MdBV (total 37 genes in 7 protein families) [10, 11, 14]. However, it is not known exactly which functional genes are expressed in virus-infected host hemocytes.

Of the few protein families common to both BV and IV, viral ankyrins (vanks), occur in members of both genera [40]. Various reports have shown that vanks function as IκB mimics, but they lack a regulatory domain for phosphorylation and ubiquitination, which could result in irreversible binding to NF-κB to inhibit an immune response [4, 7, 38, 39]. IκB-like proteins, containing ankyrin-repeat domains (Anks) that are highly similar to *Drosophila* IκB, and Cactus, have also been found in BVs, such as CcBV (8 vanks), CvBV (8 vanks), GiBV (9 vanks), GfBV (8 vanks), and MdBV (12 vanks). A recent study demonstrated that two IκB mimics, Ank-H4, and N5, from MdBV bind to *Drosophila* NF-κB factors Dorsal and Relish, whereupon the expression of several antimicrobial peptide genes is reduced [7].

NF-κB, Relish, and Dorsal share an REL homology domain (RHD), which is essential for dimerization and DNA binding [7, 16, 37]. Human NF-κB/IκB proteins contain two-antiparallel α-helices and a β-hairpin, sharing G-TPLH and LL–GA consensus repeats [28]. Although vankyrins are known to inhibit host NF-κB, their effect on host NF-κB gene expression during viral immunosuppression remains largely unclear. Induction of apoptosis is an effective immunosuppression strategy, and NF-κB/IκB signaling pathways are known to regulate cell survival and apoptosis. Thus, the transcription patterns of NF-κB/IκB in the apoptotic cells can be used to identify vankyrins that interfere with host NF-κB/IκB gene expression.

The *Microplitis bicoloratus* and *Spodoptera litura* model is an excellent system for studying immunosuppression occurring via the induction of apoptosis [25–27]. In our previously study, we showed, using gel electrophoresis, that *Microplitis bicoloratus* bracovirus (MbBV) contains at least 11 circular dsDNAs from 8 to 50 kbp [26]. MbBV-induced apoptosis against host granulocytes causes immunosuppression [25] via viral gene expression in host hemocytes [20]. Transcriptomes of non-parasitized and parasitized *S. litura* hemocytes contains sequences of host NF-κB/IκB genes, *relish*, *dorsal*, and *cactus*, and also the transcribed viral genes [20]. Importantly, the endogenous Spli221 cell line, which undergoes low-level apoptosis under normal cell culture conditions [21], allows us to generate pre-apoptotic Spli221 cells infected by MbBV particles to perform *in vitro* assays. To screen for genes expressed in apoptotic hemocytes, we performed whole-genome sequencing of MbBV and identified 116 genes. By comparing those sequences with the transcriptome of *S. litura* hemocytes parasitized by the wasp *M. bicoloratus*, we identified three IκB-like genes, *vank86*, *vank92*, and *vank101*, in 13 screened expressed genes. Then, we used a bioinformatics approach to identify NF-κB/IκB-related factors from both the host *S. litura* and BVs. Using *in vivo* and *in vitro* transcriptional analyses of these NF-κB/IκB factors, we identified potential correlations in their expression patterns. We found that viral IκB-like transcription could not inhibit host NF-κB/IκB expression at the mRNA level, suggesting that they might use different mechanisms to regulate transcription.

Materials and methods

Insect rearing and experimental animals

The *S. litura* colony was reared on an artificial diet formulated as described previously [19] at 27 ± 1 °C, RH 60-80 %, with a 12:12 h photoperiod regime. The parasitoid *M. bicoloratus* colony was maintained on *S. litura* larvae reared in the laboratory. Adults were also provided with honey as a dietary supplement. The parasitoid colony was passaged according to established methods [27].

Cell culture

Spli221 (TUAT-Spli221) adherent cells were derived from *S. litura* [29]. Cells were cultured in TNM-FH insect culture medium containing 10 % fetal bovine serum (FBS,

Hyclone). Cells were maintained at 27 °C and passaged in 25-cm^2 tissue culture flasks (Corning).

Isolation and purification of viral particles and infection of Spli221 cells

Purified viral particles were prepared based on a previously published protocol [25, 26] with minor modifications. Briefly, fresh wasps were frozen at -20 °C for 10 min and then put on ice. Reproductive tracts of female wasps were excised under a binocular stereo dissecting microscope, and separated ovaries were collected into a 2-ml tube on ice until further use. The calyces were punctured using forceps, and the calyx fluid was resuspended in 1x PBS, and then using a 2.5-ml needle, dispersed by aspirating back and forth. The mixture was centrifuged for 3 min at 1,000 *g* at 4 °C, to remove eggs and cellular debris. A 0.45-μm syringe filter was used to purify the viral particles. Two hundred thousand Spli221 cells were seeded in a 12-well culture plate (Corning) 2 h before infection. The quantity of virus used in experiments is expressed in wasp equivalents. A volume of 15 μl of purified viral particles (1.5 wasp equivalents) was added per well.

Isolation, sequencing, assembly and gene prediction of viral genomic DNA

Purified viral supernatant was centrifuged at 12,000 *g* for 15 min at 4 °C, and viral pellets were incubated in 200 μl of PDV-DNA lysis buffer (100 mM NaCl, 10 mM Tris/HCl, 25 mM EDTA, 0.5 % SDS, pH 8.0) containing 2.5 mg of proteinase K per ml, 8 μl of 20 % Sarcosyl solution, and 1 mg of RNaseA per ml at 55 °C for 3 h. The isolated DNA was further purified by phenol-chloroform extraction and subsequent ethanol precipitation. High-quality DNA samples (with an A260/A280 ratio>2.0) were further amplified using an illustra^{TM} TempliPhi kit (GE Healthcare UK) following the manufacturer's instructions. The samples were sequenced using an Illumina Hiseq 2000, and the total number of bases sequenced was greater than 3 Gbp. *De novo* DNA-seq assembly was performed using Velvet and ABySS software, respectively [34, 42]. Assembled contigs were merged, and redundant sequences were removed. GeneMark software was used to identify functional proteins from the isolated contigs [24].

PDV gene expression in hemocytes

Clean reads were mapped to assembled contigs to obtain RPM values based on read numbers [30]. Statistical analysis of data was performed using DESeq [2]. A *p*-value of 0.001 was set as the criterion for identification of significant differences in gene expression based on a previously described method [20].

Isolation of total RNA, cDNA synthesis, and qRT-PCR

Whole tiny larvae collected 1–3 days post-parasitization (p.p.), hemocytes from 4-7 days p.p. collected from parasitized *S. litura* larvae, and Spli221 cells collected 1-5 h postinfection (p.i.) were used for RNA isolation. Isolation of total RNA, cDNA synthesis, and qRT-PCR was performed as per previously published protocols [20]. The $2^{-\Delta\Delta CT}$ method was used as reported previously [22]. Three replications were carried out for each sample. Assays were repeated at least three times. Comparisons were performed using unpaired *t*-tests.

Phylogenetic and transcriptional analysis of NF-κB and IκB-like genes

The amino acid sequences of NF-κB and IκB-like proteins from *S. litura, M. bicoloratus* bracovirus, and *M. demolitor* bracovirus were retrieved from GenBank and aligned using webPRANK [23]. Alignment of NF-κB and IκB-like sequences was performed for phylogenetic analysis using the maximum-likelihood method. These analyses were performed using MEGA 6 software [17]. The transcriptional data were used for further analysis to generate a heatmap using MeV v4.9 software [33].

Statistical analysis

Comparisons between data groups were performed as stated in each figure legend using GraphPad Prism ver. 6. Differences between groups with a *p*-value less than 0.05 were considered significant. The resulting data are presented as mean ± SEM. All assays were repeated at least three times.

GenBank accession numbers

All of the sequences from this project have been deposited in the GenBank database under the accession numbers KP258410 to KP258647 and KP274920.

Results

General features of the *M. bicoloratus* bracovirus (MbBV) genome

After sequencing, a total of 7,620,970 paired reads were obtained, with 250-bp-length sequences from each pair and

a total sequence length of 3.8 Gbp. Altogether, 336,336 bp of MbBV genomic fragments were obtained from 239 reassembled scaffolds ranging in length from 500 base pairs (bp) to 15,413 bp (GenBank accession nos. KP258410-KP258647 and KP274920). In total, 116 genes were identified (Table 1), and 60 contigs were mapped to the sequenced genomes from three other bracoviruses, namely *M. demolitor* bracovirus, *C. congregata* bracovirus, and *C. sesamiae* bracovirus (CsBV). Computational comparison of the genomic organizations of the three viral genomes suggested that the genes identified in MbBV were organized in 17 putative dsDNA circles (Table 2). Therefore, the putative circles were named MbBV-C1 to C17 (Fig. 1A). The remaining contigs (F1-F179) were fragments that did not form parts of a circle (Table 1, Figs. S1, S2). Computational analysis of the putative circles and fragments revealed the presence of 50 ORFs in 15 circles (Fig. 1A) and 66 ORFs in 61 fragments (Fig. 1B).

General features of the predicted ORFs in the MbBV genome

In the MbBV genome, we identified 116 ORFs, which we numbered according to the length of the scaffold on which they were found (Table 1). Every single ORF was predicted to encode a protein of > 100 amino acids in length. In total, 14 of the putative circles contained ORFs, except circles 2 and 4, while circles 7 and 10 contained only one ORF, and circle 16, which was the largest genomic segment, contained 10 ORFs. Fragment 161 contained three ORFs, fragments 141, 142, and 155 contained two ORFs, and 57 fragments each contained only one ORF (Fig. 1B). No ORFs were found in the remaining 118 fragments (Figs. S1, S2). These 116 genes were then analyzed on the basis of the presence of conserved domains. A unique feature of the MbBV genome is the major gene families it encodes. In MbBV, nine gene families were identified. Table 3 provides an overview of the predicted proteins, together with their corresponding protein families. With 28 members, ankyrin-repeat (Vank) and protein tyrosine phosphatases (PTPs) were the two largest protein families we identified. The third-largest MbBV gene family we identified was reverse transcriptase (RT), which comprised five gene members. RT genes are a new gene family found in BVs, and their functions in these viruses are unknown. The fourth-largest MbBV gene family we identified was the Ben-domain-coding proteins, which comprise three gene members. Aminoglycoside phosphotransferase (APH), and N-methylhydantoinase (ATP hydrolyzing) are two new families found in BVs, and their functions are also unknown. The remaining three gene families, EGF-like, mucin-like (a Glc) and helicase each comprise one member. The 47 hypothetical protein members await further analysis. The genes were named by using the protein family plus gene ID, as shown in Table 4, which contains the gene ontology (GO) annotation required for further functional research. Finally, the 28 viral ankyrin genes, which are commonly shared by BVs and IVs, were similar to the IκB-like gene.

Comparative transcriptome analysis of host NF-κB/IκB and MbBV genes transcribed in apoptotic hemocytes by parasitism

The transcriptome data for hemocytes undergoing apoptosis after parasitization by *M. bicoloratus* and non-apoptotic hemocytes have been reported previously [20]. To screen for the viral genes transcribed in host hemocytes that are involved in apoptosis, we compared the 116 genes identified in MbBV with the transcriptome of host-parasitized apoptotic hemocytes. The two generated datasets revealed that 13 viral genes were expressed in the apoptotic hemocytes upon parasitism by the wasp *M. bicoloratus* (Table 5). These genes, which belong to six conserved gene families in the MbBV genome, include three *vank* genes, six *ptp* genes, one *hp* gene, one *ben* gene, one egf-like gene, and one *mucin-like* gene (Fig. 1A and B, asterisks). The three proteins that contained ankyrin-repeat domains were Vank86 in circle 14, Vank92 in circle 10, and Vank101 in circle 16 (Fig. 1A). RNAseq-based comparative analysis and hierarchical cluster analysis revealed that the abundance of mRNA for viral genes such as IκB-like, Vank86, Vank92 and Vank101 were enriched in the apoptotic hemocyte transcriptomes of parasitized *S. litura* (RPKM_M), but not in host NF-κB/IκB, Relish, Dorsal, and Cactus (Fig. 2, red asterisks).

Functional domain analysis of viral IκB-like and host NF-κB/IκB genes transcribed in apoptosis-induced hemocytes

To obtain a detailed breakdown of the Ank domains present in both virus and host, we performed a bioinformatics analysis of the different domains based on their ORF sequences. For the functional analysis, we also analyzed two Ank proteins from MdBV, namely N5 and H4, whose IκB-like functions have been studied before [38]. The phylogenetic tree obtained from the analysis followed the alignment of the two MdBV genes and the three Ank domain genes from MbBV, as well as the three host NF-κB/IκB genes, *dorsal*, *relish*, and *cactus*. As shown in Fig 3A, the phylogenetic tree was separated into two branches, one containing the two NF-κB host gene mem-

Table 1 239 scaffolds reassembled contained 116 genes

No.	Scaffolds	Length (bp)	Fragments	GenBank Accession number	Gene_ID
1	scaffold8436.1-refined	500	MbBV-F5	KP258410	gene-1
2	scaffold8425.1-refined	500	MbBV-F4	KP258411	
3	scaffold8431.1-refined	500	MbBV-F1	KP258412	
4	scaffold8434.1-refined	501	MbBV-F9	KP258413	
5	scaffold8435.1-refined	500	MbBV-F2	KP258414	
6	scaffold8410.1-refined	501	MbBV-F7	KP258415	
7	scaffold8415.1-refined	501	MbBV-F6	KP258416	
8	scaffold8419.1-refined	500	MbBV-F3	KP258417	
9	scaffold8421.1-refined	501	MbBV-F8	KP258418	
10	scaffold8394.1-refined	502	MbBV-F10	KP258419	
11	scaffold8385.1-refined	503	MbBV-F11	KP258420	
12	scaffold8355.1-refined	504	MbBV-F12	KP258421	gene-2
13	scaffold8346.1-refined	505	MbBV-F13	KP258422	
14	scaffold8334.1-refined	505	MbBV-F14	KP258423	
15	scaffold8339.1-refined	506	MbBV-F15	KP258424	
16	scaffold8298.1-refined	508	MbBV-F16	KP258425	
17	scaffold8284.1-refined	509	MbBV-F18	KP258426	
18	scaffold8293.1-refined	509	MbBV-F17	KP258427	
19	scaffold8260.1-refined	511	MbBV-F19	KP258428	
20	scaffold8213.1-refined	513	MbBV-F20	KP258429	
21	scaffold8227.1-refined	513	MbBV-F21	KP258430	
22	scaffold8197.1-refined	514	MbBV-F22	KP258431	
23	scaffold8210.1-refined	514	MbBV-C3	KP258432	gene-3
24	scaffold8172.1-refined	516	MbBV-F24	KP258433	
25	scaffold8173.1-refined	516	MbBV-F23	KP258434	gene-4
26	scaffold8178.1-refined	516	MbBV-C3	KP258435	gene-5
27	scaffold8131.1-refined	519	MbBV-F25	KP258436	
28	scaffold8071.1-refined	522	MbBV-F26	KP258437	
29	scaffold7987.1-refined	528	MbBV-F27	KP258438	gene-6
30	scaffold7961.1-refined	529	MbBV-F28	KP258439	
31	scaffold7965.1-refined	529	MbBV-F29	KP258440	
32	scaffold7936.1-refined	530	MbBV-F30	KP258441	
33	scaffold7922.1-refined	531	MbBV-F31	KP258442	gene-7
34	scaffold7911.1-refined	532	MbBV-F32	KP258443	
35	scaffold7880.1-refined	534	MbBV-F33	KP258444	gene-8
36	scaffold7869.1-refined	535	MbBV-F34	KP258445	gene-9
37	scaffold7856.1-refined	536	MbBV-F35	KP258446	
38	scaffold7793.1-refined	540	MbBV-F38	KP258447	gene-10
39	scaffold7801.1-refined	540	MbBV-F37	KP258448	gene-11
40	scaffold7756.1-refined	543	MbBV-F39	KP258449	
41	scaffold7740.1-refined	545	MbBV-F40	KP258450	gene-12
42	scaffold7723.1-refined	546	MbBV-F41	KP258451	
43	scaffold7690.1-refined	548	MbBV-F42	KP258452	
44	scaffold7671.1-refined	550	MbBV-F43	KP258453	
45	scaffold7633.1-refined	552	MbBV-F44	KP258454	
46	scaffold7642.1-refined	552	MbBV-F179	KP258455	
47	scaffold7615.1-refined	554	MbBV-F45	KP258456	
48	scaffold7603.1-refined	555	MbBV-F46	KP258457	gene-13

Table 1 continued

No.	Scaffolds	Length (bp)	Fragments	GenBank Accession number	Gene_ID
49	scaffold7556.1-refined	559	MbBV-F47	KP258458	
50	scaffold7559.1-refined	559	MbBV-F48	KP258459	
51	scaffold7513.1-refined	563	MbBV-F49	KP258460	
52	scaffold7479.1-refined	565	MbBV-F50	KP258461	
53	scaffold7449.1-refined	567	MbBV-F51	KP258462	gene-14
54	scaffold7426.1-refined	569	MbBV-F52	KP258463	
55	scaffold7389.1-refined	572	MbBV-F53	KP258464	
56	scaffold7399.1-refined	572	MbBV-F54	KP258465	gene-15
57	scaffold7380.1-refined	573	MbBV-F55	KP258466	gene-16
58	scaffold7360.1-refined	574	MbBV-F56	KP258467	
59	scaffold7320.1-refined	577	MbBV-C6	KP258468	
60	scaffold7306.1-refined	578	MbBV-F57	KP258469	
61	scaffold7280.1-refined	579	MbBV-F58	KP258470	
62	scaffold7268.1-refined	580	MbBV-F59	KP258471	gene-17
63	scaffold7253.1-refined	582	MbBV-F60	KP258472	gene-18
64	scaffold7229.1-refined	585	MbBV-F61	KP258473	
65	scaffold7209.1-refined	586	MbBV-F62	KP258474	
66	scaffold7178.1-refined	589	MbBV-F64	KP258475	
67	scaffold7179.1-refined	589	MbBV-F63	KP258476	
68	scaffold7159.1-refined	591	MbBV-F65	KP258477	gene-19
69	scaffold7146.1-refined	592	MbBV-F66	KP258478	
70	scaffold7120.1-refined	594	MbBV-F67	KP258479	
71	scaffold7053.1-refined	603	MbBV-F70	KP258480	
72	scaffold7006.1-refined	606	MbBV-F73	KP258481	
73	scaffold7008.1-refined	606	MbBV-F72	KP258482	
74	scaffold6989.1-refined	608	MbBV-C1	KP258483	
75	scaffold6979.1-refined	609	MbBV-F74	KP258484	
76	scaffold6965.1-refined	612	MbBV-F75	KP258485	
77	scaffold6931.1-refined	615	MbBV-F76	KP258486	
78	scaffold6890.1-refined	618	MbBV-F77	KP258487	
79	scaffold6877.1-refined	619	MbBV-F78	KP258488	
80	scaffold6866.1-refined	620	MbBV-F79	KP258489	
81	scaffold6870.1-refined	620	MbBV-F81	KP258490	gene-20
82	scaffold6872.1-refined	620	MbBV-F80	KP258491	
83	scaffold6774.1-refined	629	MbBV-F82	KP258492	
84	scaffold6744.1-refined	632	MbBV-F83	KP258493	gene-21
85	scaffold6750.1-refined	632	MbBV-F84	KP258494	
86	scaffold6718.1-refined	634	MbBV-F85	KP258495	
87	scaffold6666.1-refined	640	MbBV-F86	KP258496	
88	scaffold6634.1-refined	642	MbBV-F87	KP258497	gene-22
89	scaffold6628.1-refined	643	MbBV-F88	KP258498	
90	scaffold6596.1-refined	647	MbBV-F89	KP258499	gene-23
91	scaffold6589.1-refined	648	MbBV-F91	KP258500	
92	scaffold6592.1-refined	648	MbBV-F90	KP258501	gene-24
93	scaffold6526.1-refined	654	MbBV-F92	KP258502	
94	scaffold6501.1-refined	657	MbBV-C1	KP258503	gene-25
95	scaffold6492.1-refined	658	MbBV-F93	KP258504	
96	scaffold6472.1-refined	661	MbBV-F94	KP258505	gene-26

Table 1 continued

No.	Scaffolds	Length (bp)	Fragments	GenBank Accession number	Gene_ID
97	scaffold6415.1-refined	668	MbBV-F96	KP258506	gene-27
98	scaffold6253.1-refined	684	MbBV-F97	KP258507	gene-28
99	scaffold6181.1-refined	692	MbBV-F99	KP258508	gene-29
100	scaffold6162.1-refined	694	MbBV-F100	KP258509	
101	scaffold6145.1-refined	696	MbBV-F101	KP258510	
102	scaffold6133.1-refined	697	MbBV-F102	KP258511	gene-30
103	scaffold6099.1-refined	700	MbBV-F103	KP258512	gene-31
104	scaffold6083.1-refined	701	MbBV-F104	KP258513	
105	scaffold6086.1-refined	701	MbBV-F105	KP258514	
106	scaffold6088.1-refined	701	MbBV-F106	KP258515	gene-32
107	scaffold6067.1-refined	703	MbBV-F107	KP258516	
108	scaffold5948.1-refined	716	MbBV-F109	KP258517	
109	scaffold5951.1-refined	716	MbBV-F108	KP258518	
110	scaffold5781.1-refined	732	MbBV-F110	KP258519	gene-33
111	scaffold5704.1-refined	740	MbBV-F111	KP258520	gene-34
112	scaffold5646.1-refined	747	MbBV-F112	KP258521	
113	scaffold5591.1-refined	752	MbBV-F113	KP258522	gene-35
114	scaffold5528.1-refined	760	MbBV-C1	KP258523	gene-36
115	scaffold5292.1-refined	788	MbBV-F116	KP258524	
116	scaffold5280.1-refined	789	MbBV-F117	KP258525	
117	scaffold5250.1-refined	793	MbBV-F118	KP258526	gene-37
118	scaffold5076.1-refined	819	MbBV-F120	KP258527	
119	scaffold5066.1-refined	821	MbBV-F121	KP258528	
120	scaffold4982.1-refined	832	MbBV-F122	KP258529	
121	scaffold4942.1-refined	840	MbBV-F123	KP258530	gene-38
122	new_add_Contig1	573	MbBV-C3	KP274920	gene-39
123	scaffold4897.1-refined	848	MbBV-F178	KP258531	
124	scaffold4838.1-refined	858	MbBV-F124	KP258532	
125	scaffold4529.1-refined	908	MbBV-C3	KP258533	gene-40
126	scaffold4369.1-refined	813	MbBV-F119	KP258534	
127	scaffold4244.1-refined	962	MbBV-F125	KP258535	geng-41
128	scaffold3977.1-refined	1021	MbBV-F128	KP258536	
129	scaffold7928.1-refined	1041	MbBV-F130	KP258537	gene-42
130	scaffold7962.1-refined	780	MbBV-F115	KP258538	gene-43
131	scaffold7895.1-refined	597	MbBV-F68	KP258539	
132	scaffold7574.1-refined	1096	MbBV-F135	KP258540	gene-44
133	scaffold6747.1-refined	989	MbBV-F126	KP258541	
134	scaffold6278.1-refined	1049	MbBV-F132	KP258542	gene-45
135	scaffold5733.1-refined	1111	MbBV-F136	KP258543	gene-46
136	scaffold6457.1-refined	1114	MbBV-F137	KP258544	
137	scaffold5174.1-refined	1084	MbBV-F134	KP258545	
138	scaffold5024.1-refined	1044	MbBV-F131	KP258546	gene-47-1/47-2
139	scaffold5699.1-refined	1369	MbBV-F141	KP258547	gene-48/49
140	scaffold5277.1-refined	1441	MbBV-F142	KP258548	gene-50/51
141	scaffold4357.1-refined	1445	MbBV-F143	KP258549	
142	scaffold2350.1-refined	1690	MbBV-F149	KP258550	
143	scaffold3177.1-refined	1687	MbBV-F148	KP258551	
144	scaffold2209.1-refined	1786	MbBV-F150	KP258552	

Table 1 continued

No.	Scaffolds	Length (bp)	Fragments	GenBank Accession number	Gene_ID
145	scaffold5841.1-refined	1832	MbBV-F152	KP258553	
146	scaffold1894.1-refined	2092	MbBV-F156	KP258554	gene-52
147	scaffold5423.1-refined	754	MbBV-F114	KP258555	gene-53
148	scaffold3400.1-refined	1798	MbBV-F151	KP258556	
149	scaffold1387.1-refined	2857	MbBV-F161	KP258557	gene-54/55/56-1/56-2
150	scaffold2443.1-refined	2865	MbBV-F162	KP258558	gene-57
151	NODE_172_length_295_cov_2601.955811_refined	501	MbBV-C6	KP258559	
152	NODE_40_length_331_cov_502.885193_refined	537	MbBV-F36	KP258560	gene-58
153	NODE_118_length_346_cov_1246.384399_refined	552	MbBV-C5	KP258561	
154	NODE_82_length_351_cov_1500.649536_refined	557	MbBV-C6	KP258562	
155	NODE_88_length_365_cov_1217.520508_refined	571	MbBV-C6	KP258563	
156	NODE_111_length_392_cov_411.392853_refined	598	MbBV-F69	KP258564	
157	NODE_168_length_398_cov_2136.753662_refined	604	MbBV-F71	KP258565	gene-59
158	NODE_16_length_430_cov_840.597656_refined	636	MbBV-C6	KP258566	gene_id = 60
159	NODE_51_length_439_cov_390.425964_refined	645	MbBV-C16	KP258567	gene_id = 61
160	NODE_102_length_441_cov_1514.102051_refined	647	MbBV-C6	KP258568	
161	NODE_131_length_447_cov_236.046982_refined	653	MbBV-C17	KP258569	
162	NODE_52_length_458_cov_153.770737_refined	664	MbBV-F95	KP258570	
163	NODE_81_length_457_cov_2130.593018_refined	663	MbBV-C6	KP258571	
164	NODE_59_length_498_cov_254.016068_refined	704	MbBV-C6	KP258572	gene_id = 62
165	NODE_76_length_538_cov_129.291824_refined	744	MbBV-F165	KP258573	
166	NODE_62_length_553_cov_147.432190_refined	759	MbBV-C6	KP258574	
167	NODE_169_length_590_cov_387.869476_refined	796	MbBV-C4	KP258575	
168	NODE_157_length_617_cov_2013.398682_refined	823	MbBV-C6	KP258576	
169	NODE_113_length_621_cov_3059.776123_refined	827	MbBV-C6	KP258577	gene_id = 63
170	NODE_64_length_632_cov_51.246834_refined	838	MbBV-F166	KP258578	
171	NODE_74_length_701_cov_101.887306_refined	907	MbBV-F167	KP258579	
172	NODE_5_length_712_cov_808.047729_refined	918	MbBV-C16	KP258580	gene_id = 64
173	NODE_17_length_713_cov_2122.102295_refined	919	MbBV-C9	KP258581	gene_id = 65
174	NODE_107_length_811_cov_77.413071_refined	1017	MbBV-F127	KP258582	
175	NODE_100_length_817_cov_185.046509_refined	1023	MbBV-F168	KP258583	
176	NODE_31_length_825_cov_59.229092_refined	1031	MbBV-F169	KP258584	
177	NODE_140_length_824_cov_28.930826_refined	1030	MbBV-F129	KP258585	
178	NODE_94_length_833_cov_895.900391_refined	1039	MbBV-C16	KP258586	gene_id = 66
179	NODE_154_length_835_cov_26.221558_refined	1041	MbBV-F170	KP258587	
180	NODE_73_length_854_cov_146.770493_refined	1060	MbBV-F171	KP258588	
181	NODE_26_length_870_cov_166.334488_refined	1076	MbBV-F133	KP258589	
182	NODE_84_length_949_cov_329.473145_refined	1155	MbBV-F138	KP258590	
183	NODE_119_length_960_cov_742.260437_refined	1166	MbBV-C14	KP258591	
184	NODE_61_length_979_cov_274.851898_refined	1185	MbBV-F172	KP258592	gene-67
185	NODE_63_length_1085_cov_121.013824_refined	1291	MbBV-F139	KP258593	
186	NODE_27_length_1090_cov_398.298157_refined	1296	MbBV-F140	KP258594	gene-68
187	NODE_38_length_1250_cov_165.799194_refined	1456	MbBV-F144	KP258595	gene-69
188	NODE_112_length_1255_cov_78.690041_refined	1461	MbBV-F173	KP258596	
189	NODE_105_length_1292_cov_288.479095_refined	1498	MbBV-F145	KP258597	
190	NODE_136_length_1359_cov_81.830025_refined	1565	MbBV-F146	KP258598	
191	NODE_11_length_1372_cov_1130.352051_refined	1578	MbBV-C4	KP258599	
192	NODE_67_length_1384_cov_99.178467_refined	1590	MbBV-F174	KP258600	gene_id = 70

Table 1 continued

No.	Scaffolds	Length (bp)	Fragments	GenBank Accession number	Gene_ID
193	NODE_41_length_1419_cov_151.180405_refined	1625	MbBV-F175	KP258601	gene_id = 71
194	NODE_90_length_1461_cov_981.085571_refined	1667	MbBV-C14	KP258602	gene_id = 72
195	NODE_78_length_1523_cov_600.885742_refined	1729	MbBV-C14	KP258603	
196	NODE_85_length_1541_cov_1485.420532_refined	1747	MbBV-C5	KP258604	gene_id = 73
197	NODE_58_length_1600_cov_248.709381_refined	1806	MbBV-C7	KP258605	
198	NODE_77_length_1656_cov_47.950481_refined	1862	MbBV-F176	KP258606	
199	NODE_86_length_1675_cov_294.212524_refined	1881	MbBV-F153	KP258607	
200	NODE_80_length_1684_cov_151.956650_refined	1890	MbBV-F154	KP258608	
201	NODE_56_length_1787_cov_257.673187_refined	1993	MbBV-F155	KP258609	gene-74/75
202	NODE_98_length_1884_cov_1090.253662_refined	2090	MbBV-C4	KP258610	
203	NODE_92_length_1923_cov_650.736328_refined	2129	MbBV-F157	KP258611	gene-76
204	NODE_20_length_1925_cov_694.494568_refined	2131	MbBV-C14	KP258612	gene-77
205	NODE_57_length_1966_cov_729.953735_refined	2172	MbBV-C10	KP258613	
206	NODE_95_length_2024_cov_1345.843384_refined	2230	MbBV-C14	KP258614	gene-78
207	NODE_43_length_2131_cov_288.591278_refined	2337	MbBV-F158	KP258615	gene-79
208	NODE_93_length_2195_cov_1234.465576_refined	2401	MbBV-C5	KP258616	gene-80
209	NODE_126_length_2267_cov_20.909573_refined	2473	MbBV-F177	KP258617	gene-81
210	NODE_68_length_2323_cov_140.375809_refined	2529	MbBV-F159	KP258618	
211	NODE_70_length_2389_cov_208.144409_refined	2595	MbBV-F160	KP258619	
212	NODE_44_length_2541_cov_321.803619_refined	2747	MbBV-C7	KP258620	gene-82
213	NODE_10_length_2556_cov_1527.051270_refined	2762	MbBV-C9	KP258621	gene-83
214	NODE_7_length_2764_cov_243.326706_refined	2970	MbBV-F163	KP258622	gene-84
215	NODE_4_length_2890_cov_1813.898315_refined	3096	MbBV-C9	KP258623	gene-85
216	NODE_25_length_3156_cov_689.371033_refined	3362	MbBV-C14	KP258624	gene-86
217	NODE_83_length_3216_cov_349.123444_refined	3422	MbBV-C13	KP258625	
218	NODE_50_length_3425_cov_827.212280_refined	3631	MbBV-C14	KP258626	
219	NODE_6_length_3431_cov_558.906433_refined	3637	MbBV-C16	KP258627	gene-87
220	NODE_36_length_3579_cov_162.718079_refined	3785	MbBV-C7	KP258628	
221	NODE_21_length_4035_cov_1303.600220_refined	4241	MbBV-C9	KP258629	
222	NODE_54_length_4511_cov_718.168030_refined	4717	MbBV-C16	KP258630	gene-88/89
223	NODE_9_length_4777_cov_352.034760_refined	4983	MbBV-F164	KP258631	gene-90
224	NODE_14_length_4861_cov_617.472534_refined	5067	MbBV-C17	KP258632	gene-91
225	NODE_49_length_4897_cov_732.217712_refined	5103	MbBV-C10	KP258633	gene-92
226	NODE_34_length_5114_cov_665.664429_refined	5320	MbBV-C10	KP258634	
227	NODE_22_length_5312_cov_293.235687_refined	5518	MbBV-C13	KP258635	gene-93
228	NODE_47_length_5590_cov_354.114838_refined	5796	MbBV-C13	KP258636	gene-94
229	NODE_45_length_6052_cov_733.558350_refined	6258	MbBV-C12	KP258637	gene-95/96
230	NODE_28_length_8012_cov_753.555542_refined	8218	MbBV-C12	KP258638	gene-97/98
231	NODE_18_length_8132_cov_284.994476_refined	8338	MbBV-C16	KP258639	gene-99/100/101/102
232	NODE_8_length_9461_cov_1586.392700_refined	9667	MbBV-C8	KP258640	gene-103/104/105
233	NODE_3_length_10741_cov_419.980621_refined	10947	MbBV-C17	KP258641	gene-106
234	NODE_65_length_12564_cov_46.433460_refined	12770	MbBV-C11	KP258642	gene-107/108/109/110/111/112/113
235	NODE_13_length_15207_cov_443.688904_refined	15413	MbBV-C15	KP258643	gene-114/115
236	other_NODE_2256_length_489_cov_11.292434_refined	689	MbBV-F98	KP258644	
237	other_NODE_785_length_719_cov_25.956884_refined	918	MbBV-C14	KP258645	
238	other_NODE_384_length_1462_cov_439.419281_refined	1662	MbBV-F147	KP258646	gene-116
239	other_NODE_4911_length_2111_cov_42.166271_refined	2311	MbBV-C2	KP258647	

Table 2 17 putative dsDNA circles of *M. bicoloratus* bracovirus

Circle	Contig	Gene_ID	ref_length	identify	alignment_len	SNP	INDEL
MbBV-C1	scaffold6989.1-refined		41573	93.98	83	5	0
	scaffold6501.1-refined	gene_id = 25	41573	82.08	385	69	0
	scaffold5528.1-refined	gene_id = 36	41573	90.85	142	13	0
MbBV-C2	other_NODE_4911_length_2111_cov_42.166271_refined		99167	94.8	846	40	3
	other_NODE_4911_length_2111_cov_42.166271_refined		99167	96.08	102	4	0
	other_NODE_4911_length_2111_cov_42.166271_refined		99167	94.97	597	30	0
MbBV-C3	scaffold8178.1-refined	gene_id = 5	30655	83.1	213	36	0
	scaffold4529.1-refined	gene_id = 40	30655	83.85	650	105	0
	scaffold8210.1-refined	gene_id = 3	30655	84.78	289	44	0
	new_add_Contig1	gene_id = 39	30655	84.62	156	24	0
	new_add_Contig1		30655	84.62	182	28	0
	new_add_Contig1		30655	84.5	413	64	0
	new_add_Contig1		30655	88.08	151	18	0
MbBV-C4	NODE_169_length_590_cov_387.869476_refined		4576	90.22	808	59	7
	NODE_98_length_1884_cov_1090.253662_refined		4576	90.5	484	44	1
	NODE_98_length_1884_cov_1090.253662_refined		4576	89.05	1196	98	10
	NODE_11_length_1372_cov_1130.352051_refined		4576	90.88	1085	84	4
MbBV-C5	NODE_93_length_2195_cov_1234.465576_refined	gene_id = 80	3611	91.62	1313	98	6
	NODE_93_length_2195_cov_1234.465576_refined		3611	92.22	257	19	1
	NODE_85_length_1541_cov_1485.420532_refined	gene_id = 73	3611	88.64	880	95	5
	NODE_85_length_1541_cov_1485.420532_refined		3611	86.26	575	60	1
	NODE_118_length_346_cov_1246.384399_refined		3611	90.96	188	16	1
MbBV-C6	NODE_16_length_430_cov_840.597656_refined	gene_id = 60	7228	92.92	438	31	0
	scaffold7320.1-refined		7228	93.51	570	33	1
	NODE_82_length_351_cov_1500.649536_refined		7228	88.77	285	25	3
	NODE_82_length_351_cov_1500.649536_refined		7228	92.41	158	12	0
	NODE_81_length_457_cov_2130.593018_refined		7228	91.12	608	44	3
	NODE_62_length_553_cov_147.432190_refined		7228	94.46	397	22	0
	NODE_62_length_553_cov_147.432190_refined		7228	89.43	227	20	2
	NODE_113_length_621_cov_3059.776123_refined	gene_id = 63	7228	92.37	826	63	0
	NODE_59_length_498_cov_254.016068_refined	gene_id = 62	7228	92.08	707	49	4
	NODE_102_length_441_cov_1514.102051_refined		7228	89.77	665	46	8
	NODE_172_length_295_cov_2601.955811_refined		7228	91.24	502	29	4
	NODE_157_length_617_cov_2013.398682_refined		7228	91.21	819	66	5
	NODE_88_length_365_cov_1217.520508_refined		7228	91.83	575	40	4
MbBV-C7	NODE_58_length_1600_cov_248.709381_refined		6307	95.56	248	11	0
	NODE_58_length_1600_cov_248.709381_refined		6307	91.09	651	53	3
	NODE_44_length_2541_cov_321.803619_refined	gene_id = 82	6307	88.36	1538	159	5
	NODE_44_length_2541_cov_321.803619_refined		6307	85.7	748	91	4
	NODE_36_length_3579_cov_162.718079_refined		6307	90.45	1204	110	3
	NODE_36_length_3579_cov_162.718079_refined		6307	93.98	216	13	0
MbBV-C8	NODE_8_length_9461_cov_1586.392700_refined	gene_id = 103	9604	92.23	605	47	0
	NODE_8_length_9461_cov_1586.392700_refined	gene_id = 104	9604	90.73	464	40	2
	NODE_8_length_9461_cov_1586.392700_refined	gene_id = 105	9604	92.39	276	19	2
	NODE_8_length_9461_cov_1586.392700_refined		9604	90.01	2902	255	9
	NODE_8_length_9461_cov_1586.392700_refined		9604	90.71	1335	122	2
	NODE_8_length_9461_cov_1586.392700_refined		9604	90.92	2103	186	4
	NODE_8_length_9461_cov_1586.392700_refined		9604	84.73	203	28	1
	NODE_8_length_9461_cov_1586.392700_refined		9604	87.94	456	51	3

Table 2 continued

Circle	Contig	Gene_ID	ref_length	identify	alignment_len	SNP	INDEL
MbBV-C9	NODE_21_length_4035_cov_1303.600220_refined		10790	87.96	357	43	0
	NODE_21_length_4035_cov_1303.600220_refined		10790	91.28	814	55	6
	NODE_21_length_4035_cov_1303.600220_refined		10790	94.01	217	10	1
	NODE_21_length_4035_cov_1303.600220_refined		10790	91.65	934	73	3
	NODE_21_length_4035_cov_1303.600220_refined		10790	91.51	1390	112	5
	NODE_4_length_2890_cov_1813.898315_refined	gene_id = 85	10790	90.49	3113	268	10
	NODE_10_length_2556_cov_1527.051270_refined	gene_id = 83	10790	90.92	1498	109	13
	NODE_10_length_2556_cov_1527.051270_refined		10790	91.63	1111	89	3
	NODE_17_length_713_cov_2122.102295_refined	gene_id = 65	10790	92.27	919	68	1
MbBV-C10	NODE_57_length_1966_cov_729.953735_refined		13279	86.97	376	41	1
	NODE_57_length_1966_cov_729.953735_refined		13279	89.68	1676	139	7
	NODE_49_length_4897_cov_732.217712_refined	gene_id = 92	13279	90.39	2113	191	9
	NODE_49_length_4897_cov_732.217712_refined		13279	89.79	676	68	1
	NODE_49_length_4897_cov_732.217712_refined		13279	88.61	1106	122	3
	NODE_49_length_4897_cov_732.217712_refined		13279	91.94	856	67	2
	NODE_34_length_5114_cov_665.664429_refined		13279	89.57	2166	217	6
	NODE_34_length_5114_cov_665.664429_refined		13279	90.04	562	56	0
	NODE_34_length_5114_cov_665.664429_refined		13279	92.28	803	55	2
	NODE_34_length_5114_cov_665.664429_refined		13279	87.18	117	15	0
	NODE_34_length_5114_cov_665.664429_refined		13279	90.4	125	12	0
	NODE_34_length_5114_cov_665.664429_refined		13279	91.23	912	73	4
MbBV-C11	NODE_65_length_12564_cov_46.433460_refined	gene_id = 107	11238	95.19	208	10	0
	NODE_65_length_12564_cov_46.433460_refined	gene_id = 108	11238	81.89	773	140	0
	NODE_65_length_12564_cov_46.433460_refined	gene_id = 109	11238	92.73	2147	132	7
	NODE_65_length_12564_cov_46.433460_refined	gene_id = 110	11238	90.91	1309	118	1
	NODE_65_length_12564_cov_46.433460_refined	gene_id = 111	11238	92.43	2073	147	5
	NODE_65_length_12564_cov_46.433460_refined	gene_id = 112	11238	90.59	776	61	2
	NODE_65_length_12564_cov_46.433460_refined	gene_id = 113	11238	94.1	712	42	0
	NODE_65_length_12564_cov_46.433460_refined		11238	93.91	1674	91	4
MbBV-C12	NODE_28_length_8012_cov_753.555542_refined	gene_id = 97	15218	88.65	229	26	0
	NODE_28_length_8012_cov_753.555542_refined	gene_id = 98	15218	89.13	2630	269	11
	NODE_28_length_8012_cov_753.555542_refined		15218	91.47	914	75	2
	NODE_28_length_8012_cov_753.555542_refined		15218	92.75	1599	110	6
	NODE_28_length_8012_cov_753.555542_refined		15218	93.11	755	49	2
	NODE_28_length_8012_cov_753.555542_refined		15218	90.19	581	43	4
	NODE_28_length_8012_cov_753.555542_refined		15218	91.67	1320	93	2
	NODE_45_length_6052_cov_733.558350_refined	gene_id = 95	15218	95.9	268	11	0
	NODE_45_length_6052_cov_733.558350_refined	gene_id = 96	15218	90.66	3920	317	17
	NODE_45_length_6052_cov_733.558350_refined		15218	93.06	418	27	2
	NODE_45_length_6052_cov_733.558350_refined		15218	85.62	459	54	3
	NODE_45_length_6052_cov_733.558350_refined		15218	91.32	334	28	1
MbBV-C13	NODE_22_length_5312_cov_293.235687_refined	gene_id = 93	15058	87.37	594	60	6
	NODE_22_length_5312_cov_293.235687_refined		15058	88.62	2162	221	14
	NODE_22_length_5312_cov_293.235687_refined		15058	91.71	1025	76	5
	NODE_22_length_5312_cov_293.235687_refined		15058	88.75	391	42	2
	NODE_22_length_5312_cov_293.235687_refined		15058	89.23	520	42	6
	NODE_22_length_5312_cov_293.235687_refined		15058	88.06	310	36	1
	NODE_83_length_3216_cov_349.123444_refined		15058	89.57	1496	143	10
	NODE_83_length_3216_cov_349.123444_refined		15058	88.64	1936	199	11
	NODE_47_length_5590_cov_354.114838_refined	gene_id = 94	15058	94.01	167	10	0

Table 2 continued

Circle	Contig	Gene_ID	ref_length	identify	alignment_len	SNP	INDEL
	NODE_47_length_5590_cov_354.114838_refined		15058	90.37	696	64	2
	NODE_47_length_5590_cov_354.114838_refined		15058	89.89	2314	217	8
	NODE_47_length_5590_cov_354.114838_refined		15058	89.81	569	55	3
	NODE_47_length_5590_cov_354.114838_refined		15058	86.24	1010	126	5
MbBV-C14	NODE_78_length_1523_cov_600.885742_refined		13704	89.57	968	87	8
	NODE_20_length_1925_cov_694.494568_refined	gene_id = 77	13704	87.96	324	37	1
	NODE_20_length_1925_cov_694.494568_refined		13704	92.09	645	51	0
	NODE_25_length_3156_cov_689.371033_refined		13704	91.7	1639	109	5
	NODE_25_length_3156_cov_689.371033_refined	gene_id = 86	13704	93.07	231	16	0
	NODE_25_length_3156_cov_689.371033_refined		13704	92.54	362	26	1
	other_NODE_785_length_719_cov_25.956884_refined		13704	90.83	109	10	0
	NODE_119_length_960_cov_742.260437_refined		13704	90.62	469	42	2
	NODE_119_length_960_cov_742.260437_refined		13704	88.15	346	38	2
	NODE_90_length_1461_cov_981.085571_refined	gene_id = 72	13704	91.35	1422	107	6
	NODE_50_length_3425_cov_827.212280_refined		13704	88.21	1137	124	5
	NODE_50_length_3425_cov_827.212280_refined		13704	89.46	1480	154	2
	NODE_50_length_3425_cov_827.212280_refined		13704	90.8	87	7	1
	NODE_50_length_3425_cov_827.212280_refined		13704	93.2	147	10	0
	NODE_95_length_2024_cov_1345.843384_refined	gene_id = 78	13704	90.46	2181	167	12
MbBV-C15	NODE_13_length_15207_cov_443.688904_refined	gene_id = 114	15096	85.98	371	27	4
	NODE_13_length_15207_cov_443.688904_refined	gene_id = 115	15096	91.04	1607	140	4
	NODE_13_length_15207_cov_443.688904_refined		15096	90.56	339	31	1
	NODE_13_length_15207_cov_443.688904_refined		15096	89.03	1668	171	8
	NODE_13_length_15207_cov_443.688904_refined		15096	89.27	708	49	3
	NODE_13_length_15207_cov_443.688904_refined		15096	89.09	1045	83	6
	NODE_13_length_15207_cov_443.688904_refined		15096	91.09	449	37	3
	NODE_13_length_15207_cov_443.688904_refined		15096	91.97	4000	306	9
	NODE_13_length_15207_cov_443.688904_refined		15096	91.13	203	18	0
	NODE_13_length_15207_cov_443.688904_refined		15096	90.6	1064	98	2
	NODE_13_length_15207_cov_443.688904_refined		15096	87.63	1099	127	6
	NODE_13_length_15207_cov_443.688904_refined		15096	89.71	894	67	5
	NODE_13_length_15207_cov_443.688904_refined		15096	89.87	750	66	5
MbBV-C16	NODE_54_length_4511_cov_718.168030_refined	gene_id = 88	17355	89.74	809	78	4
	NODE_54_length_4511_cov_718.168030_refined	gene_id = 89	17355	90.89	417	35	2
	NODE_54_length_4511_cov_718.168030_refined		17355	91.27	573	44	4
	NODE_54_length_4511_cov_718.168030_refined		17355	87.08	1184	113	12
	NODE_54_length_4511_cov_718.168030_refined		17355	90.01	1351	122	6
	NODE_51_length_439_cov_390.425964_refined	gene_id = 61	17355	95.04	645	31	1
	NODE_18_length_8132_cov_284.994476_refined	gene_id = 100	17355	90.19	2906	233	16
	NODE_18_length_8132_cov_284.994476_refined	gene_id = 101	17355	83.78	524	85	0
	NODE_18_length_8132_cov_284.994476_refined	gene_id = 102	17355	81.9	232	38	1
	NODE_18_length_8132_cov_284.994476_refined	gene_id = 99	17355	88.07	696	78	2
	NODE_18_length_8132_cov_284.994476_refined		17355	84.16	202	24	3
	NODE_6_length_3431_cov_558.906433_refined	gene_id = 87	17355	88.43	527	50	6
	NODE_6_length_3431_cov_558.906433_refined		17355	91.19	2487	176	15
	NODE_94_length_833_cov_895.900391_refined	gene_id = 66	17355	92.46	1048	70	2
	NODE_5_length_712_cov_808.047729_refined	gene_id = 64	17355	92.12	926	62	8
MbBV-C17	NODE_131_length_447_cov_236.046982_refined		7823	82.91	398	50	9
	NODE_14_length_4861_cov_617.472534_refined	gene_id = 91	7823	89.77	2375	225	8
	NODE_14_length_4861_cov_617.472534_refined		7823	90.31	320	30	1

Table 2 continued

Circle	Contig	Gene_ID	ref_length	identify	alignment_len	SNP	INDEL
	NODE_14_length_4861_cov_617.472534_refined		7823	90.3	1299	118	2
	NODE_3_length_10741_cov_419.980621_refined	gene_id = 106	7823	89	782	78	4
	NODE_3_length_10741_cov_419.980621_refined		7823	89.83	354	28	2
	NODE_3_length_10741_cov_419.980621_refined		7823	92.86	98	7	0
	NODE_3_length_10741_cov_419.980621_refined		7823	91.8	793	57	5

Circle	contig_start	contig_end	ref_start	ref_end	E_value	Score	Reference
MbBV-C1	524	606	15080	14998	4.00E-29	125	*C. congregata* bracovirus segment Circle32
	135	519	15414	15030	1.00E-56	216	
	576	717	15624	15483	4.00E-45	178	
MbBV-C2	201	1044	71284	72127	0.00E+00	1306	*C. sesamiae Mombasa* bracovirus clone BAC 6I18
	1319	1420	72124	72225	3E-42	170	
	1519	2115	72956	73552	0.00E+00	946	
MbBV-C3	18	230	25135	24923	9.00E-33	137	*C. congregata* bracovirus segment Circle31
	247	896	25173	25822	1.00E-128	456	
	8	296	25713	26001	5.00E-59	224	
	1	156	26281	26436	5.00E-27	119	
	336	517	26255	26436	5.00E-33	139	
	553	965	26483	26895	6.00E-85	311	
	991	1141	26598	26748	2.00E-38	157	
MbBV-C4	1	796	648	1447	0	946	*M. demolitor* bracovirus segment E
	2	483	1450	1933	3.00E-168	589	
	909	2090	2204	3380	0	1298	
	479	1554	4569	3491	0	1356	
MbBV-C5	850	2150	1	1313	0	1695	*M. demolitor* bracovirus segment A
	2140	2396	1333	1588	2.00E-95	347	
	10	885	1585	2463	0	924	
	883	1457	2607	3162	5.00E-154	541	
	186	373	3611	3425	8.00E-61	230	
MbBV-C6	1	438	83	520	7.00E-179	622	*M. demolitor* bracovirus segment C
	8	577	497	1062	0	839	
	1	282	1246	1526	1.00E-81	299	
	400	557	1547	1704	3.00E-57	218	
	9	615	2145	1547	0	767	
	5	401	2246	2642	5.00E-177	617	
	530	755	2644	2867	5.00E-66	248	
	2	827	2953	3778	0	1142	
	2	704	4276	3573	0	932	
	1	646	4366	5027	0	743	
	2	501	5518	5030	0	636	
	6	823	5526	6339	0	1015	
	1	568	6523	7097	0	741	
MbBV-C7	1269	1516	248	1	8.00E-113	404	*M. demolitor* bracovirus segment B
	373	1022	1310	664	0	811	
	1213	2747	3015	1495	0	1628	
	186	931	3750	3017	2.00E-179	626	
	652	1853	4017	5217	0	1455	
	2234	2449	5979	6194	1.00E-88	325	

Table 2 continued

Circle	contig_start	contig_end	ref_start	ref_end	E_value	Score	Reference
MbBV-C8	702	1306	1	605	0	827	*M. demolitor* bracovirus segment F
	1888	2348	642	1105	2.00E-160	565	
	2569	2842	1102	1377	4.00E-100	365	
	2907	5797	1387	4264	0	3433	
	6071	7405	4262	5594	0	1647	
	7569	9667	5613	7714	0	2625	
	3	205	8950	9149	3.00E-36	153	
	248	701	9151	9604	1.00E-124	446	
MbBV-C9	3853	4209	10784	10428	4.00E-101	367	*M. demolitor* bracovirus segment G
	3038	3846	803	1	0	1027	
	2398	2611	1171	955	6.00E-88	323	
	1400	2332	2146	1217	0	1213	
	1	1386	3594	2207	0	1782	
	1	3096	3603	6704	0	3780	
	1	1488	6805	8285	0	1816	
	1649	2757	8410	9518	0	1443	
	1	916	9447	10365	0	1255	
MbBV-C10	1695	2070	368	1	3.00E-100	363	*M. demolitor* bracovirus segment I
	1	1663	2027	373	0	1957	
	3000	5103	4135	2026	0	2518	
	2079	2754	6465	5791	0	785	
	977	2078	7679	6574	0	1172	
	62	915	8560	7705	0	1134	
	428	2589	8433	10593	0	2464	
	2613	3174	10590	11151	0	670	
	3262	4057	11152	11954	0	1094	
	4055	4171	12009	12125	1.00E-24	113	
	4222	4346	12138	12262	2.00E-36	153	
	4415	5320	12268	13178	0	1152	
MbBV-C11	1711	1918	211	4	2.00E-90	333	*M. demolitor* bracovirus segment H
	5958	6730	2134	1362	3.00E-117	422	
	10635	12770	4557	2424	0	2997	
	9321	10629	5932	4625	0	1643	
	7204	9267	8082	6011	0	2835	
	4956	5730	8633	7869	0	963	
	3732	4443	9512	8801	0	1078	
	1922	3592	11238	9573	0	2492	
MbBV-C12	1	229	8853	9081	5.00E-65	248	*M. demolitor* bracovirus segment M
	229	2844	9232	11858	0	2870	
	2886	3798	11859	12770	0	1179	
	3804	5397	12847	14444	0	2202	
	5664	6415	14463	15217	0	1070	
	6248	6818	1	577	0	688	
	6899	8218	583	1885	0	1758	
	1	268	1680	1947	3.00E-124	444	
	273	4186	2596	6472	0	4797	
	4258	4673	6791	7208	6.00E-166	583	
	5478	5928	7226	7680	4.00E-105	381	
	5926	6258	8562	8895	3.00E-118	424	

Table 2 continued

Circle	contig_start	contig_end	ref_start	ref_end	E_value	Score	Reference
MbBV-C13	4772	5363	11455	10875	3.00E-158	557	*M. demolitor* bracovirus segment K
	2630	4771	13780	11624	0	2246	
	1610	2631	14854	13836	0	1326	
	859	1249	393	5	4.00E-114	410	
	324	834	1576	1062	1.00E-157	555	
	1	309	1928	1619	7.00E-85	313	
	1939	3422	3341	1847	0	1655	
	7	1934	5314	3392	0	2042	
	4913	5079	6137	5971	2.00E-66	252	
	5097	5792	5857	5165	0	842	
	2033	4340	8708	6406	0	2686	
	1440	2006	9269	8702	0	644	
	10	1015	10269	9269	0	876	
MbBV-C14	771	1727	970	6	0	1066	*M. demolitor* bracovirus segment J
	924	1245	1375	1698	2.00E-89	327	
	1484	2128	1703	2347	0	874	
	1745	3362	4175	2543	0	2179	
	612	842	4411	4181	2.00E-90	331	
	205	565	4824	4463	6.00E-140	496	
	1	109	4995	5103	2.00E-32	137	
	698	1166	5666	5200	2.00E-161	565	
	170	515	6070	5728	1.00E-95	347	
	91	1505	7485	6073	0	1816	
	2439	3569	8774	7642	0	1162	
	747	2224	10439	8960	0	1681	
	369	455	10807	10722	3.00E-21	101	
	504	650	10721	10575	1.00E-54	212	
	79	2230	13704	11536	0	2637	
MbBV-C15	10034	10400	350	1	2.00E-90	333	*M. demolitor* bracovirus segment L
	8342	9946	1972	368	0	2012	
	7899	8237	2457	2120	1.00E-113	410	
	6239	7902	4157	2498	0	1800	
	5538	6219	4903	4197	0	825	
	4520	5534	5978	4935	0	1170	
	4043	4489	6428	5981	2.00E-155	549	
	1	3995	10423	6434	0	5325	
	15179	15381	11207	11005	3.00E-68	260	
	14049	15111	12277	11215	0	1300	
	12679	13776	13461	12371	0	1059	
	11290	12163	14347	13459	0	1043	
	10416	11155	15096	14347	0	854	
MbBV-C16	178	983	13	819	0	916	*M. demolitor* bracovirus segment N
	1112	1526	821	1236	8.00E-146	515	
	1543	2115	1223	1789	0	716	
	2156	3311	1803	2974	0	1094	
	3376	4717	2995	4341	0	1574	
	2	645	4192	4836	0	1017	
	5462	8338	7798	4916	0	3457	
	4025	4548	8952	8429	3.00E-100	365	
	4682	4913	11432	11205	5.00E-28	125	

Table 2 continued

Circle	contig_start	contig_end	ref_start	ref_end	E_value	Score	Reference
	2976	3671	12266	11576	0	712	
	1402	1595	12681	12480	2.00E-30	133	
	622	1138	12496	13021	3.00E-148	523	
	1171	3637	13134	15597	0	3134	
	1	1039	16439	15392	0	1453	
	3	918	17355	16431	0	1203	
MbBV-C17	266	653	859	1248	6.00E-53	204	*M. demolitor* bracovirus segment D
	135	2498	1177	3544	0	2753	
	2494	2812	3566	3885	3.00E-105	381	
	2812	4102	3916	5214	0	1572	
	8415	9193	5300	6076	0	844	
	9192	9537	6114	6467	2.00E-114	412	
	9809	9906	6667	6764	5.00E-32	139	
	7574	8361	7823	7034	0	1023	

bers, and one containing all of the other genes that are related to IκB (Fig. 3A, left), and the gene domains based on the ORFs are also shown (Fig. 3A, right). Host IκB Cactus contained 10 Ank domains: three Ank, three Ank2, and four Ank4. Vank92 and H4 contain two Ank domains. Vank101, N5, and Vank86 contain four Ank domains. Host Relish contains three Ank2 and two Ank domains, the N-terminal subdomain of the RHD, which is involved in DNA binding, and the IPT domain of the transcription factor NF-κB and the death domain of NF-κB precursor proteins. Host Dorsal does not harbor an Ank domain, but it contains an MADF, DNA-binding domain at its N-terminus and a BESS motif at its C-terminus. All Ank domains were separated from host IκB and viral IκB-like and then aligned. For the IκB branch, the Ank superfamily, which contains two antiparallel α-helices and a β-hairpin [28], was aligned and the similar consensus sequence (-LL–GAD/N, -G-TPLH-) identified may be involved in the formation of α-helices (Fig. 2B). A similar analysis of the viral proteins shows that Vank86 contains three Ank domains and one Ank2 domain, and that Vank92 contains two overlapping Ank domains, while Vank101 contains two Ank and two Ank2 domains. However, none of these viral proteins contain an RHD, suggesting that their role might be similar to that of IκB (i.e. an inhibitor of NF-κB function). Two specific domains, IPT_NF-κB in the N-terminus and Death_NF-κB in the C-terminus of Relish, are shown in Fig. 3C. Taken together, these results suggest that Vank86, Vank92, and Vank101 from MbBV and H4, and N5 from MdBV are highly similar in their overall sequences, and importantly, they share the same Ank motifs. This indicates that they are likely to act as viral IκB mimics.

Molecular interactions between host and virus with respect to NF-κB signaling in apoptotic hemocytes

To investigate the expression patterns of both host and viral genes of the NF-κB/IκB family in apoptotic hemocytes, we compared the mRNA expression levels for both viral IκB-like and host NF-κB/IκB genes. Total RNA from larvae at 1-3 days post-parasitization (p.p.), as well as from the apoptotic hemocytes at 4-7 days p.p., was isolated, and qRT-PCR was performed (Table 6, Figs. S3-S9). Fig. 4A shows how host NF-κB Relish increased from 1 to 3 days p.p. However, no significant differences were seen in the mRNA levels among the samples from 4, 5, 6 and 7 days p.p.. By comparison, host Dorsal showed a statistically significant decrease between days 1 and 2 p.p. (Fig. 4B). The Dorsal mRNA level in the apoptosis-induced hemocytes was relatively stable, with no significant differences observed for days 4 to 7 p.p.. For host IκB Cactus, the hemocyte mRNA level increased markedly between days 4 and 7 p.p., and the mRNA levels in the larvae from days 1 to 3 p.p. were consistently stable (Fig. 4C). The viral IκB-like Vank86 had significantly lower mRNA levels in larvae on days 1 and 2 p.p. compared with the levels on days 3 p.p. onwards (Fig. 4D). In contrast, the mRNA expression levels of the viral IκB-like genes Vank92 and Vank101 were maintained at a stable level from days 1 to 3 p.p. (Fig. 4D-F). Three of the IκB-likes (Vank86, Vank92, and Vank101) maintained relatively stable levels from days 4 to 7 p.p. (Fig. 4D-F). Together, these results suggest that viral IκB-like genes and host NF-κB/IκB genes are expressed at the same time, which also suggests that viral IκB-like genes did not inhibit the mRNA level of host NF-

Table 3 Features of the *M. bicoloratus* bracovirus protein families

Parameter	MbBV families									
	Vank	PTP	RT	Ben	Egf-like	Mucin-like	Helicase	APH	HYD	HP
Number of related genes	28	28	5	3	1	1	1	1	1	47
Circle/Fragment no. of related genes	C6:1	C11:6	C1:1	C7:1	F131:1	C17:1	F123:1	F102:1	F156:1	C1:1
	C8:1	C14:3	C3:3	F23:1						C3:1
	C9:2	C16:6	F37:1							C5:2
	C10:1	F27:1								C6:2
	C11:1	F31:1								C8:2
	C14:1	F55:1								C9:1
	C16:4	F59:1								C12:4
	F12:1	F60:1								C13:2
	F33:1	F71:1								C15:2
	F40:1	F81:1								C17:1
	F54:1	F97:1								F5:1
	F89:1	F114:1								F34:1
	F90:1	F130:1								F36:1
	F94:1	F140:1								F46:1
	F96:1	F172:1								F51:1
	F99:1	F177:1								F65:1
	F106:1									F83:1
	F110:1									F87:1
	F111:1									F103:1
	F132:1									F113:1
	F136:1									F115:1
	F141:1									F118:1
	F157:1									F125:1
	F158:1									F135:1
										F141:1
										F142:2
										F144:1
										F147:1
										F155:2
										F161:3
										F162:1
										F163:1
										F164:1
										F174:1
										F175:1
BVs in which similar gene families are found	MdBV	MdBV	None	MdBV	MdBV	MdBV	CvBV	None	None	
	CcBV	CcBV		CcBV						
	CvBV	CvBV		CvBV						
	GiBV	GiBV		GiBV						
	GfBV	GfBV		GfBV						
	TnBV	TnBV								

PTP: protein tyrosine phosphatase; Vank: viral ankyrin; RT: reverse transcriptase; Ben: Ben domain; Egf-like: epidermal growth factor-like; Mucin-like(glc): glcosylated central domain proteins; Helicase, atp-dependent dna helicase; APH: aminoglycoside phosphotransferase; HYD: N-methylhydantoinase (ATP-hydrolysing); HP: Hypothetical protein

Table 4 116 genes in *M. bicoloratus* bracovirus

Protein family + gene ID	annotation	GO	GO annotaion
HP1	hypothetical protein	0	-
Vank2	viral ankyrin	1	P:suppression by virus of host NF-kappaB transcription factor activity
RT3	reverse transcriptase, putative	3	F:RNA binding; P:RNA-dependent DNA replication; F:RNA-directed DNA polymerase activity
Ben4	ben domain-containing protein	0	-
HP5	hypothetical protein	0	-
PTP6	ptp 4	2	F:protein tyrosine phosphatase activity; P:peptidyl-tyrosine dephosphorylation
PTP7	ptp 4	2	F:protein tyrosine phosphatase activity; P:peptidyl-tyrosine dephosphorylation
Vank8	viral ankyrin 1	1	P:suppression by virus of host NF-kappaB transcription factor activity
HP9	hypothetical protein	3	F:RNA binding; P:RNA-dependent DNA replication; F:RNA-directed DNA polymerase activity
Ben10	ben domain-containing protein	0	-
RT11	reverse transcriptase, putative	3	F:RNA binding; P:RNA-dependent DNA replication; F:RNA-directed DNA polymerase activity
Vank12	viral ankyrin 1	1	P:suppression by virus of host NF-kappaB transcription factor activity
HP13	hypothetical protein	0	-
HP14	hypothetical protein	3	F:RNA binding; P:RNA-dependent DNA replication; F:RNA-directed DNA polymerase activity
Vank15	viral ankyrin 1	1	P:suppression by virus of host NF-kappaB transcription factor activity
PTP16	ptp 2	2	F:protein tyrosine phosphatase activity; P:peptidyl-tyrosine dephosphorylation
PTP17	ptp 4	2	F:protein tyrosine phosphatase activity; P:peptidyl-tyrosine dephosphorylation
PTP18	protein tyrosine phosphatase	1	P:dephosphorylation
HP19	hypothetical protein	0	-
PTP20	ptp 2	2	F:protein tyrosine phosphatase activity; P:peptidyl-tyrosine dephosphorylation
HP21	hypothetical protein	0	-
HP22	hypothetical protein	0	-
Vank23	viral ankyrin 1	1	P:suppression by virus of host NF-kappaB transcription factor activity
Vank24	viral ankyrin 1	1	P:suppression by virus of host NF-kappaB transcription factor activity
RT25	reverse transcriptase, putative	3	F:RNA binding; P:RNA-dependent DNA replication; F:RNA-directed DNA polymerase activity
Vank26	vankyrin-b1	0	-
Vank27	viral ankyrin 3	1	P:suppression by virus of host NF-kappaB transcription factor activity
PTP28	ptp 4	2	F:protein tyrosine phosphatase activity; P:peptidyl-tyrosine dephosphorylation

Table 4 continued

Protein family + gene ID	annotation	GO	GO annotaion
Vank29	viral ankyrin 2	1	P:suppression by virus of host NF-kappaB transcription factor activity
APH30	aminoglycoside phosphotransferase	2	P:protein phosphorylation; F:protein tyrosine kinase activity
HP31	hypothetical protein	0	-
Vank32	viral ankyrin 2	1	P:suppression by virus of host NF-kappaB transcription factor activity
Vank33	viral ankyrin 1	1	P:suppression by virus of host NF-kappaB transcription factor activity
Vank34	viral ankyrin 2	1	P:suppression by virus of host NF-kappaB transcription factor activity
HP35	hypothetical protein	0	-
HP36	hypothetical protein	3	F:RNA binding; P:RNA-dependent DNA replication; F:RNA-directed DNA polymerase activity
HP37	hypothetical protein	0	-
Helicase38	atp-dependent dna helicase	5	F:nucleic acid binding; F:ATP-dependent DNA helicase activity; F:ATP binding; P:DNA recombination; P:DNA repair
RT39	reverse transcriptase, putative	3	F:RNA binding; P:RNA-dependent DNA replication; F:RNA-directed DNA polymerase activity
RT40	reverse transcriptase, putative	3	F:RNA binding; P:RNA-dependent DNA replication; F:RNA-directed DNA polymerase activity
HP41	hypothetical protein	0	-
PTP42	ptp 4	2	F:protein tyrosine phosphatase activity; P:peptidyl-tyrosine dephosphorylation
HP43	hypothetical protein 2	0	-
HP44	conserved hypothetical protein	0	-
Vank45	viral ankyrin 1	1	P:suppression by virus of host NF-kappaB transcription factor activity
Vank46	viral ankyrin 2	1	P:suppression by virus of host NF-kappaB transcription factor activity
Egf47	egf1.5	1	P:suppression by virus of host innate immune response
HP48	hypothetical protein	0	-
Vank49	viral ankyrin 1	1	P:suppression by virus of host NF-kappaB transcription factor activity
HP50	hypothetical protein	0	-
HP51	hypothetical protein	0	-
HYD52	n-methylhydantoinase a	0	-
PTP53	ptp 2	2	F:protein tyrosine phosphatase activity; P:peptidyl-tyrosine dephosphorylation
HP54	hypothetical protein	0	-
HP55	hypothetical protein	0	-
HP56	hypothetical protein	0	-
HP57	hypothetical protein	0	-
HP58	hypothetical protein	0	-
TPT59	ptp 1	2	F:protein tyrosine phosphatase activity; P:peptidyl-tyrosine dephosphorylation
Vank60	viral ankyrin 1	1	P:suppression by virus of host NF-kappaB transcription factor activity

Table 4 continued

Protein family + gene ID	annotation	GO	GO annotaion
PTP61	ptp 2	2	F:protein tyrosine phosphatase activity; P:peptidyl-tyrosine dephosphorylation
HP62	hypothetical protein	0	-
HP63	hypothetical protein	0	-
PTP64	ptp	1	P:dephosphorylation
Vank65	viral ankyrin 2	1	P:suppression by virus of host NF-kappaB transcription factor activity
PTP66	ptp 1	2	F:protein tyrosine phosphatase activity; P:peptidyl-tyrosine dephosphorylation
PTP67	ptp 1	2	F:protein tyrosine phosphatase activity; P:peptidyl-tyrosine dephosphorylation
PTP68	ptp	5	F:phosphatase activity; P:dephosphorylation; P:protein dephosphorylation; P:peptidyl-tyrosine dephosphorylation; F:protein tyrosine phosphatase activity
HP69	hypothetical protein	0	-
HP70	hypothetical protein	0	-
HP71	hypothetical protein	0	-
PTP72	ptp 3	2	F:protein tyrosine phosphatase activity; P:peptidyl-tyrosine dephosphorylation
HP73	hypothetical protein 2	0	-
HP74	hypothetical protein	0	-
HP75	hypothetical protein	0	-
Vank76	viral ankyrin 1	1	P:suppression by virus of host NF-kappaB transcription factor activity
PTP77	ptp 1	2	F:protein tyrosine phosphatase activity; P:peptidyl-tyrosine dephosphorylation
PTP78	ptp 2	2	F:protein tyrosine phosphatase activity; P:peptidyl-tyrosine dephosphorylation
Vank79	viral ankyrin 3	1	P:suppression by virus of host NF-kappaB transcription factor activity
HP80	hypothetical protein	0	-
PTP81	protein tyrosine phosphatase	0	-
Ben82	ben domain-containing protein	0	-
Vank83	viral ankyrin 1	1	P:suppression by virus of host NF-kappaB transcription factor activity
HP84	hypothetical protein	0	-
HP85	hypothetical protein 2	0	-
Vank86	viral ankyrin 1	2	P:modulation by virus of host morphology or physiology; P:suppression by virus of host NF-kappaB transcription factor activity
PTP87	ptp 1	2	F:protein tyrosine phosphatase activity; P:peptidyl-tyrosine dephosphorylation
PTP88	protein tyrosine phosphatase	1	P:dephosphorylation
Vank89	viral ankyrin 3	1	P:suppression by virus of host NF-kappaB transcription factor activity
HP90	hypothetical protein	0	-
HP91	hypothetical protein 1	0	-
Vank92	viral ankyrin	1	P:suppression by virus of host NF-kappaB transcription factor activity
HP93	hypothetical protein	0	-
HP94	hypothetical protein	0	-
HP95	hypothetical protein 4	0	-

Table 4 continued

Protein family + gene ID	annotation	GO	GO annotaion
HP96	hypothetical protein	0	-
HP97	hypothetical protein 5	0	-
HP98	hypothetical protein 2	0	-
Vank99	vankyrin-b1	0	-
Vank100	viral ankyrin 2	1	P:suppression by virus of host NF-kappaB transcription factor activity
Vank101	viral ankyrin 1	1	P:suppression by virus of host NF-kappaB transcription factor activity
PTP102	protein tyrosine phosphatase	2	P:protein dephosphorylation; F:phosphoprotein phosphatase activity
HP103	hypothetical protein	0	-
HP104	hypothetical protein	0	-
Vank105	viral ankyrin 2	1	P:suppression by virus of host NF-kappaB transcription factor activity
Mucin106	glc1.8, mucin-like protein	1	P:modulation by virus of host morphology or physiology
PTP107	ptp 1	2	F:protein tyrosine phosphatase activity; P:peptidyl-tyrosine dephosphorylation
PTP108	ptp 4	2	F:protein tyrosine phosphatase activity; P:peptidyl-tyrosine dephosphorylation
PTP109	ptp 3	3	P:peptidyl-tyrosine dephosphorylation; P:suppression by virus of host innate immune response; F:protein tyrosine phosphatase activity
PTP110	ptp 1	2	P:protein dephosphorylation; F:phosphatase activity
Vank111	viral ankyrin	1	P:suppression by virus of host NF-kappaB transcription factor activity
PTP112	ptp 3	3	P:peptidyl-tyrosine dephosphorylation; P:suppression by virus of host innate immune response; F:protein tyrosine phosphatase activity
PTP113	ptp 2	5	C:host cell cytoplasm; F:protein tyrosine phosphatase activity; P:peptidyl-tyrosine dephosphorylation; P:suppression by virus of host innate immune response; P:induction by virus of host cysteine-type endopeptidase activity involved in apoptotic process
HP114	hypothetical protein	0	-
HP115	hypothetical protein	0	-
HP116	hypothetical protein	0	-

κB/IκB during wasp larvae development in the virus-induced apoptotic hemocytes in the host hemocoel.

Host-virus molecular interactions with respect to NF-κB signaling in Spli221 pre-apoptotic cells

To investigate further the expression patterns in the early infection stage between viral IκB-like and host NF-κB/IκB proteins in a virus-induced apoptotic cell population, we isolated fresh MbBV particles and use them to directly infect Spli221 cells derived from *S. litura* [41], a process that allowed us to generate a pre-apoptotic cell population with which to perform *in vitro* assays. Total RNA, isolated from cells at 1-5 h postinfection (p.i.), was subjected to qRT-PCR. The expression pattern of host NF-κB from Relish decreased significantly from 1 h to 2 h p.i. and from 4 h to 5 h p.i. (Fig. 5A). In contrast, host NF-κB mRNA levels from Dorsal (Fig. 5B) and host IκB from Cactus (Fig. 5C) did not differ significantly. Fig. 5D shows that viral IκB-like Vank86 mRNA levels significantly increased between the 1 h and 3 h samples and between 1 h and 4 h samples p.i. Intriguingly, viral IκB-like Vank101 mRNA levels between 1 h and 3 h and between 1 h and 4 h p.i. decreased significantly (Fig. 5E). However, no expression of viral IκB-like Vank92 was observed over the short time period of infection. Importantly, these results suggest that

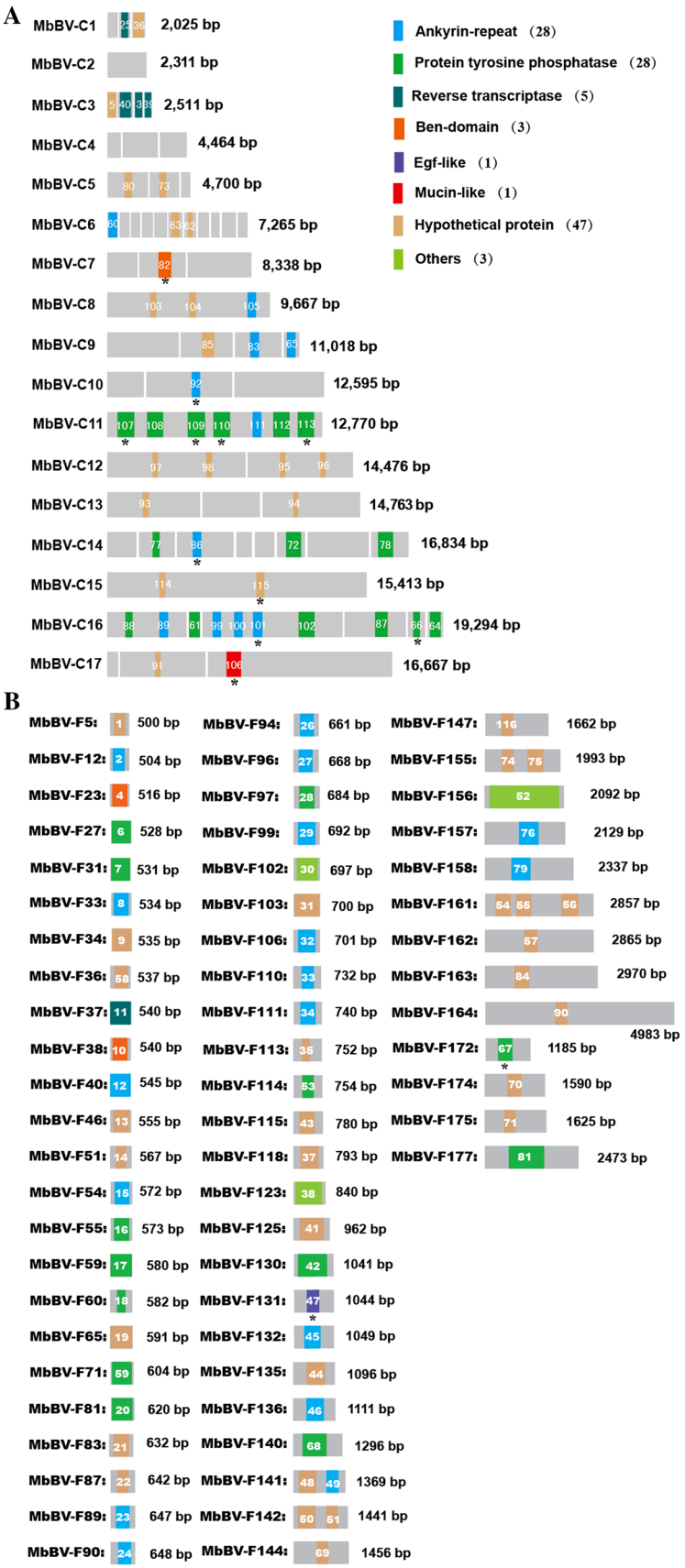

Fig. 1 The genome of *M. bicoloraus* bracovirus. The diagram represents the properties of genomic fragments of MbBV. Seventeen potential circular segments containing 50 unigenes (A) and 61 out of a total 179 fragments, containing 66 viral genes, (B) are shown. The numbers in brackets indicate the number of genes, while asterisks indicate viral genes expressed in hemocytes of *S. litura* parasitized by *M. bicoloratus*

Table 5 13 genes transcription of *M. bicoloratus* bracovirus in host hemocytes

Gene	ID_All	read_A	RPKM_A	read_B	RPKM_B	log2 (Fold_change) normalized	q-value (Benjamini et al. 1995)	Result	Gene_ID in genome
vank101	comp88993_c0_seq1	122	2.084059	0.5	8.85E-03	7.879661652	1.81E-26		gene_id_101
vank86	comp103130_c0_seq1	5536	66.423844	2	2.49E-02	11.38355254	0.00E+00	up	gene_id_86
vank92	comp22910_c0_seq1	802	10.852524	0.5	7.01E-03	10.59638274	2.47E-118	up	gene_id_92
ptp109	comp437903_c0_seq1	8	0.5883796	0.5	3.81E-02	3.948924314	8.54E-03		gene_id_109
ptp113	comp203729_c0_seq1	22	1.4011323	0.5	3.30E-02	5.408355933	2.92E-06		gene_id_113
ptp113	comp32817_c0_seq1	25	0.8450885	0.5	1.75E-02	5.592780504	5.73E-07		gene_id_113
ptp113	comp19633_c0_seq1	40	1.9750384	0.5	2.56E-02	6.270852409	2.27E-10		gene_id_113
ptp107	comp385483_c0_seq1	8	0.6222245	0.5	4.03E-02	3.948924314	8.54E-03		gene_id_107
ptp107	comp26283_c0_seq1	23	1.1718561	0.5	2.64E-02	5.47248627	1.69E-06		gene_id_107
ptp110	comp176489_c0_seq1	22	1.5165197	0.5	3.57E-02	5.408355933	2.92E-06		gene_id_110
ptp110	comp204803_c0_seq1	26	1.082995	0.5	2.16E-02	5.649364032	3.35E-07		gene_id_110
ptp66	comp8526_c0_seq1	18	0.9144542	0.5	2.63E-02	5.118849316	2.66E-05		gene_id_66
ptp67	comp82039_c0_seq1	23	1.0107259	0.5	2.28E-02	5.47248627	1.69E-06		gene_id_67
hp115	comp92227_c0_seq1	321	6.6148736	0.5	1.07E-02	9.275353801	5.50E-58	up	gene_id_115
ben82	comp93741_c0_seq4	127	2.832977	0.5	1.16E-02	7.937609001	2.32E-27		gene_id_82
mucin106 (glc1.8)	comp118173_c0_seq1	258	14.772258	0.5	2.97E-02	8.96015157	1.04E-48	up	gene_id_106
mucin106 (glc1.8)	comp85587_c0_seq1	789	40.552389	0.5	2.66E-02	10.5728058	7.26E-117	up	gene_id_106
egf47 (egf1.5)	comp99098_c0_seq1	8585	166.56266	5	1.01E-01	10.69459864	0.00E+00	up	gene_id_47

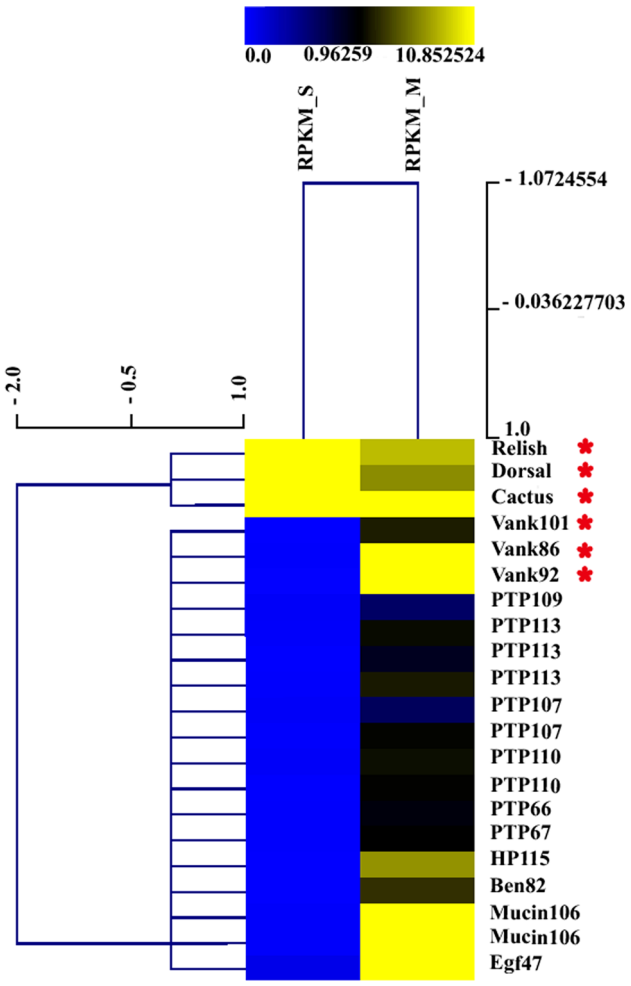

Fig. 2 Comparative transcriptome analysis of the viral IκB-like genes and host NF-κB/IκB hemocytes in which apoptosis was induced by natural parasitism. Hierarchical cluster analysis shows NF-κB/IκB and viral IκB-like genes transcribed in the hemocytes of *S. litura* (RPKM_S) and hemocytes parasitized by *M. bicoloratus* (RPKM_M). RPKM: Reads per kilobase of exon model per million mapped reads. Red asterisks show the host NF-κB, Relish, Dorsal, and Cactus and viral IκB-like, Vank86, Vank92, and Vank101

the viral IκB-like genes Vank86 and Vank101 are transcribed with host NF-κB/IκB at the same time soon after infection with MbBV particles. This result implies that viral IκB-like mRNA does not inhibit host NF-κB/IκB mRNA expression and that viral IκB-like genes and host NF-κB/IκB genes may use different transcription mechanisms.

Discussion

Polydnavirus transcription is thought to result from the interactions between host nuclear transcription factors and viral genes, the latter of which are believed to exist on a DNA fragment integrated into the host cells [5]. In this

Fig. 3 Analysis of functional domains of viral IκB-like genes and host NF-κB/IκB. (A) Phylogenetic tree of the NF-κB/IκB and IκB-like family built using MeV software and Mega6. The maximum-likelihood tree was built on the basis of NF-κB/IκB and IκB-like domains. The amino acids clustering together were divided into two distinct subclasses: NF-κB, Relish, and Dorsal from *S. litura*; IκB, Cactus from *S. litura*, IκB-like, Vank86, Vank92 and Vank101 from *M. bicoloratus* bracovirus; and H4 and N5 from *M. demolitor* bracovirus. (B) Alignment of Ank domains of NF-κB/IκB and IκB-like proteins. Two antiparallel α-helices similar to the consensus sequences are shown. (C) NF-κB domains in Relish: an IPT_NF-κB domain at the N-terminus and a Death_NF-κB domain at the C-terminus. (D) DNA binding domains in Dorsal: MADF_DNA_bdg at the N-terminus and a BESS motif in the C-terminal

study, we performed whole-genome sequencing of MbBV, and based on the computational bioinformatics analysis of its genome, 116 genes were identified, 28 of which belong to the ankyrin-repeat family. Only three viral IκB-like genes among the 13 screened genes were expressed in bracovirus-induced apoptotic hemocytes. Consequently, host NF-κB/IκB, *relish*, *dorsal*, and *cactus* genes, and viral IκB-like *vank86*, *vank92*, and *vank101* genes were each expressed in apoptosis-induced cells in a time-dependent manner. Our results suggest that viral IκB-like gene transcription did not inhibit the transcription of host NF-κB/IκB genes, suggesting that transcription of these host and viral genes have different mechanisms of regulation.

Our genomic structure analysis, which was based on Illumina Hiseq 2000 data, revealed that MbBV contains 17 potential circular dsDNA molecules of 2-20 kbp. These findings update previous expectations that MbBV possibly contains 11 circular dsDNAs with size ranges from 8-50 kbp, which were based on results obtained from gel electrophoresis [26]. In the MbBV genome, a total of 116 genes (Table 3) were identified and the existence of at least nine protein families was confirmed; furthermore, the data are mostly consistent with the data from our previously published transcriptome study, with the exception of the C-type lectin family [20]. Twenty-eight *vank* genes in the ORF sequence belonged to the ankyrin-repeat family, which is one of the largest gene families in MbBV. We also identified PTP in MbBV, and likewise in the congeneric MdBV, PTP and ankyrin-repeat proteins were also two of the largest gene families [40].

Table 1 shows the 13 genes screened by comparing 116 genes from the MbBV genome with the transcriptional data from hemocytes in which apoptosis had been induced by natural parasitism. The genes with mRNA expression confirmed in apoptotic hemocytes of the host on day 5 p.p. encoded six protein domains, including ankyrin-repeat, PTP, HP, BEN, Mucin-like and EGF domains, but not the RT family. One explanation for the differences observed in the transcriptional data for the genomic genes is that tissue-dependent and time-dependent transcriptional variations

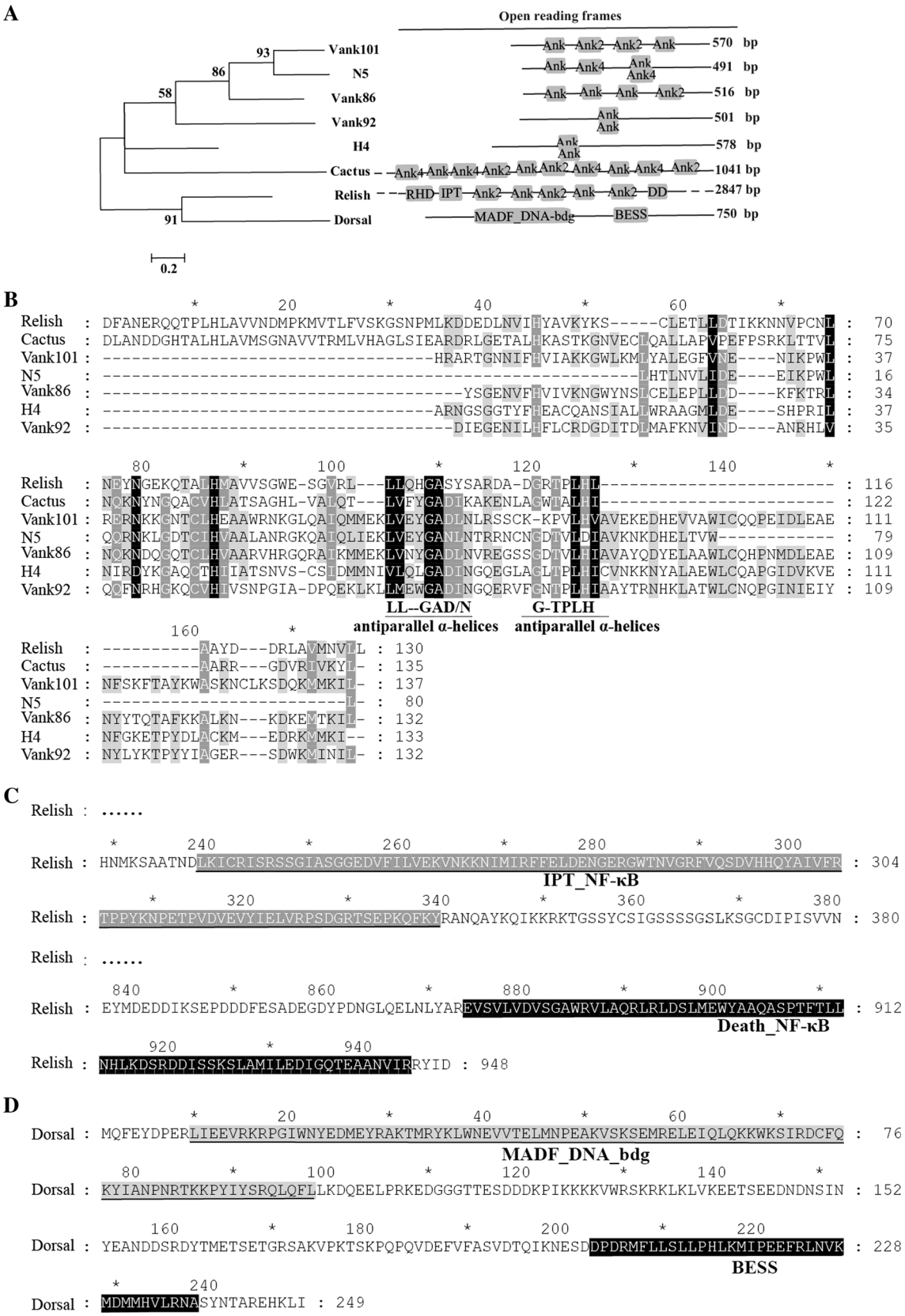
A
Open reading frames
Vank101
N5
Vank86
Vank92
H4
Cactus
Relish
Dorsal
93
86
58
91
0.2
570 bp
491 bp
516 bp
501 bp
578 bp
1041 bp
2847 bp
750 bp
Ank
Ank2
Ank4
RHD
IPT
DD
MADF_DNA-bdg
BESS
B
LL--GAD/N
antiparallel α-helices
G-TPLH
antiparallel α-helices
C
IPT_NF-κB
Death_NF-κB
D
MADF_DNA_bdg
BESS

Table 6 Primers

Gene	Forward primer (5′-3′)	Reverse primer (5′-3′)	length (bp)
relish	ATGTCTACGAGCGCCAGTGACC	TCAATCAATGTACCTTCTGATAACATTG	2847
cactus	ATGAGTGGAAATAAGAGCAAC	TCAGTACCCCTTCACCGT	1041
dorsal	ATGCAGTTCGAATACGATCCC	TTAAATCAACTTGTGTTCTCTAGCG	750
vank86	ATGGGTGTTTTAGATCTTCTAGTTC	TCAGAAAAACTTTCTTCGCAGT	516
vank92	ATGGCGCCTCCGGAAGAAA	TTAATGGCTAGTAAATAACCAAGCTTC	501
vank101	GGATCCATGGATAGCTCAGATAGTT	AAGCTTACAAACTTCGAGGTACTGA	570
Q-relish	ATGGCGGTGGTGTCT	CGATTTCGCTAGGAGGT	169
Q-cactus	GTGCCCGAACCTGCTA	GAGGTGATACGGCGATG	157
Q-dorsal	CATTCGGGACTGCTT	CCTCTTTGCGTGGTAA	119
Q-vank86	CTCAGACGGCGTTCA	TCGCAGTAGCCAGACA	107
Q-vank92	CCTCTGCCGTGATG	CGAAAACTCGCTCTTG	206
Q-vank101	CCTTAGACTGGGAGCGACAT	ACGCTGCTTCGTGGAGG	173

exist in the MbBV polydnavirus. One example of this is the eight previously identified CvBV-IκBs that have different tissue- and time-dependent transcriptional patterns [4]. Furthermore, these transcriptional patterns are consistent with our results, where virus-induced apoptotic hemocytes revealed the nature of parasitism in a short time scale of infection in the virus-induced pre-apoptosis endogenous Spli221 cell line infected by MbBV particles, as shown by the different transcription patterns for *vank86*, *vank92*, and *vank101*. Three *vank* genes were expressed in hemocytes, but not all of them were expressed in endogenous Spli221 cells; Spli221 cells are derived from the pupal ovaries of *S. litura* [29] and *vank92* was not detected in them. At this point, a question arises about whether the PDV genome had integrated into the host cell DNA. Concerning integrated DNA fragments, Beck et al. confirmed that MdBV fragments C and J can integrate into the CiE1 cell line, which is a *Pseudoplusia includens* hemocyte-derived cell line [5]. As shown in Table 2, MbBV-C14, which contains *vank86*, mapped to MdBV fragment J, while MbBV-C16, which contains *vank101*, mapped to MdBV fragment I. We propose that the two contigs, NODE_25_length_3156_cov_689.371033_refined (which contains *vank86*) and NODE_18_length_8132_cov_284.994476_refined (which contains *vank101*), but not NODE_49_length_4897_cov_732.217712_refined (which contains *vank92*, is distributed in MbBV-C10, and maps to MdBV fragment N) can integrate into endogenous Spli221 cells over a short time scale of infection; however, the transcriptional control region still needs further exploration.

Upon parasitism, certain host genes are downregulated, while others are upregulated. In *S. litura* larvae infected with MbBV, 2,441 genes were downregulated, and 299 genes were upregulated; these included viral genes at 5 days p.p. [20]. These results raise a very interesting question: does viral ankyrin inhibit host NF-κB/IκB and thereby reduce host gene expression? To address this question, we identified three NF-κB/IκB factors from the host (Fig. 3A). These factors have high sequence similarities to IκB Cactus in *Drosophila* and were initially found to inhibit Dorsal [18]. Viral ankyrin proteins appear on the same branch of the phylogenetic tree as Cactus, which is responsible for Dorsal inhibition. Relish is regulated by an upstream molecular IκB kinase [13, 31]. Chinchore et al. reported that Relish regulates cell death in retinal degeneration in *Drosophila* and that this involved activation of its N-terminal domains as a toxin, suggesting that the activated form of Relish is related to the cell apoptosis pathway [9]. Additionally, in a *Drosophila* model of ataxia-telangiectasia, constitutively activated Relish is found to be necessary for neurodegeneration [32]. At this point, polydnaviruses may trigger the activation of Relish, but further assays may need to be performed to confirm this possibility. In *Drosophila*, a loss-of-function mutant of the COP9 signalosome subunit 5 causes the co-localization of Cactus and Dorsal to the nucleus and represses Dorsal-dependent transcriptional activity [18]. In alliance with Cactus, PDV might not directly affect activated Cactus, and our data support this point. There have been several reports of PDV-regulated host NF-κB/IκB at the protein level, but here, we focused on mRNA levels during transcription. In fact, the persistent expression of both proteins, viral IκB-like and host NF-κB/IκB, suggested that the viral IκB-like protein could not inhibit the transcription of NF-κB/IκB.

Normally, we would consider that the viral IκB-like protein hijacks host NF-κB to express its own genes in much the same way that other viruses do. Examples of host NF-κB participation in the viral transcription process

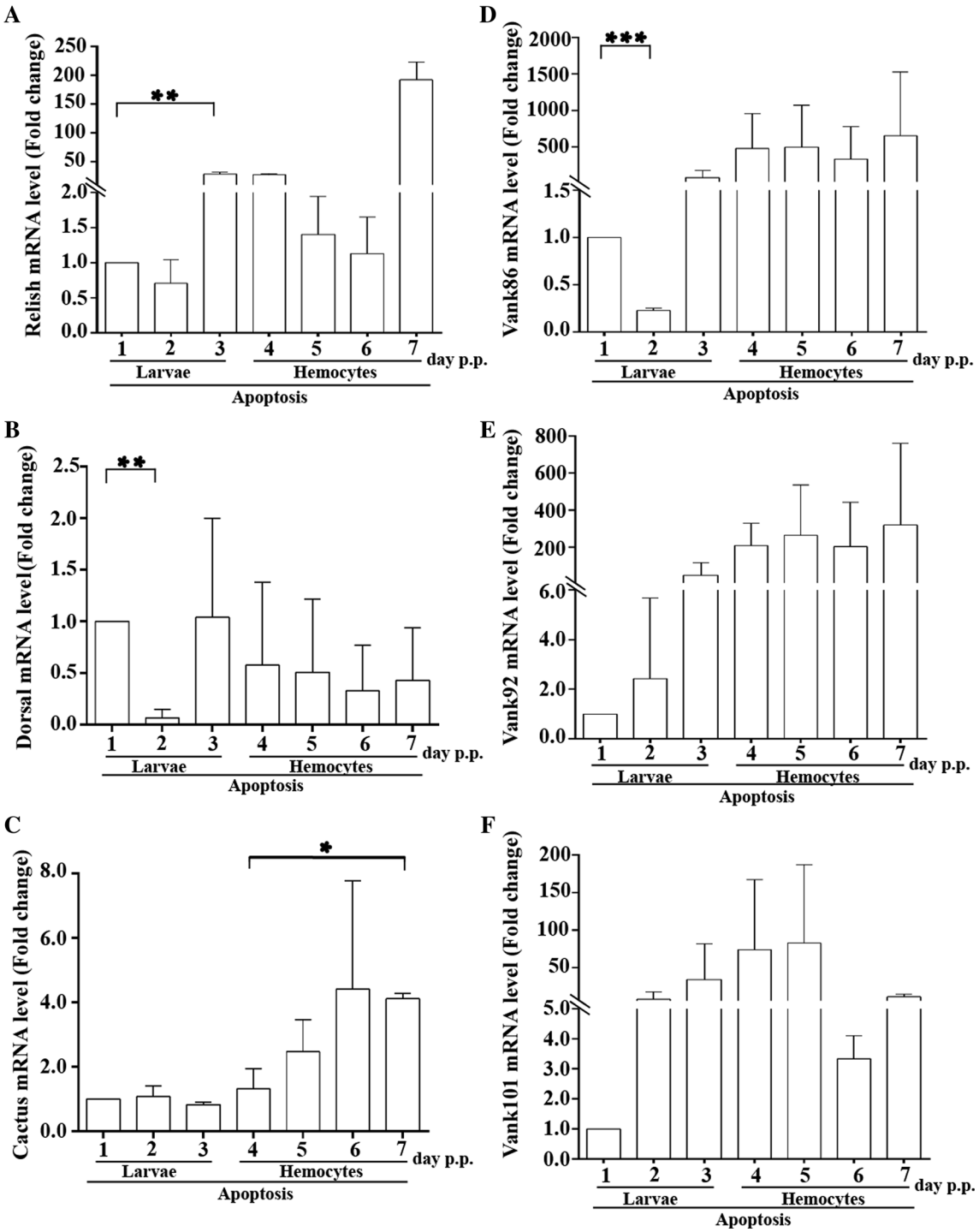

Fig. 4 Expression patterns of viral IκB-like genes and NF-κB/IκB in hemocytes in which apoptosis was induced by natural parasitism. Quantitative real-time PCR analysis was performed from 1 to 7 days post-parasitization (p.p.). Normalized mRNA levels (fold change) of Relish (A), Dorsal (B), Cactus (C), Vank86 (D), Vank92 (E), and Vank101 (F) are shown. Data are shown as mean ± SEM. Comparisons were performed using unpaired *t*-tests. 1 day p.p. compared with 2 and 3 day p.p. of parasitized larvae, and 4 day p.p. compared with 5 to 7 day p.p. of parasitized hemocytes, respectively. * indicates $p < 0.05$. ** indicates $p < 0.01$. *** indicates $p < 0.001$

include herpesvirus (human cytomegalovirus, HCMV) (dsDNA), papillomavirus (human papillomavirus type 16) (dsDNA), polyomavirus (simian virus 40, SV40) (dsDNA), and retrovirus (HIV type I) (ssRNA: dsDNA form integrates into the host genome). NF-κB is utilized to enhance the transcription of viral genes [15].

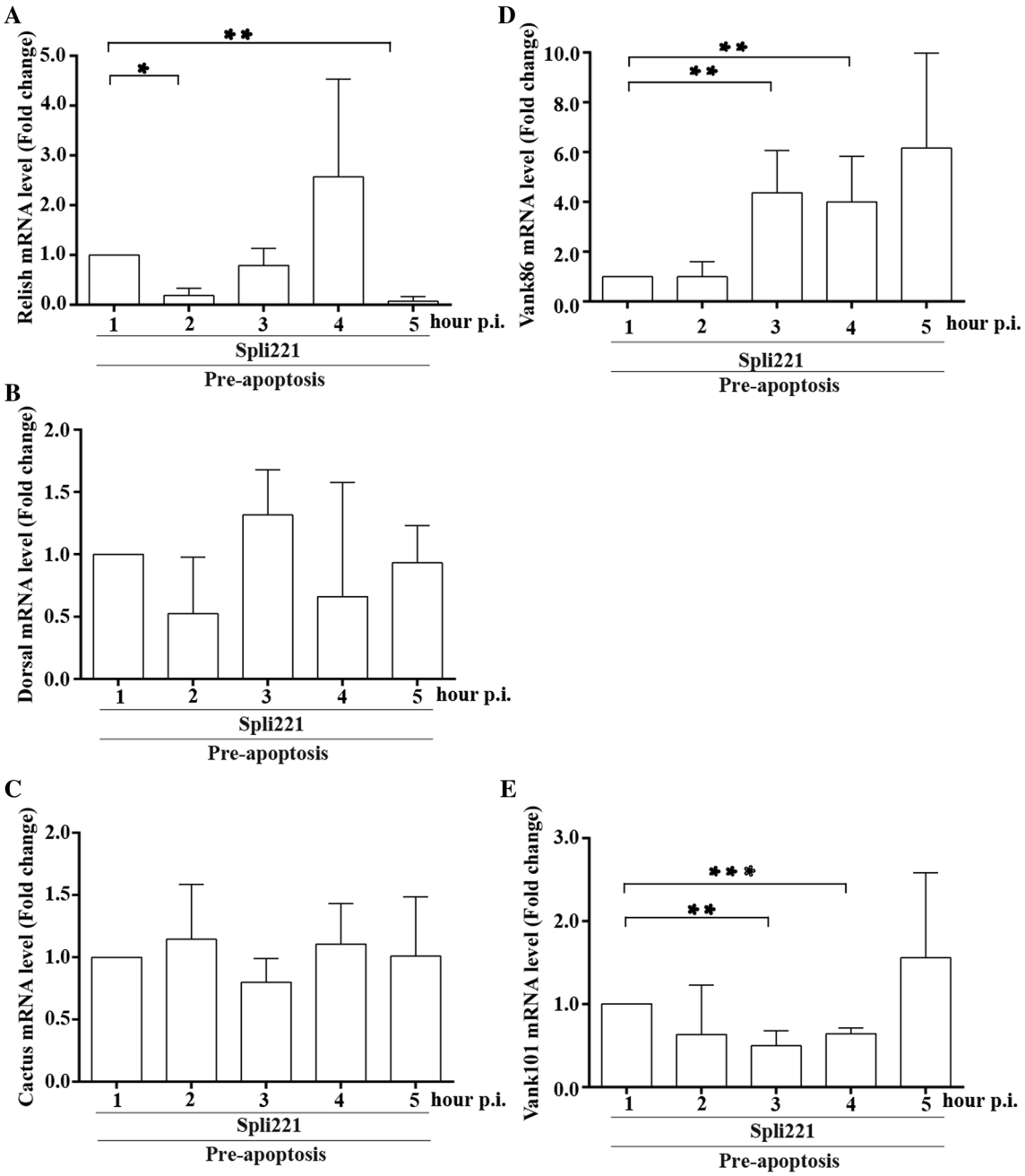

Fig. 5 Expression patterns of viral IκB-like genes and NF-κB/IκB Spli221 cells in which pre-apoptosis was induced by infection with MbBV particles. Quantitative real-time PCR analysis was performed from 1 to 5 hours postinfection (p.i.). Normalized mRNA levels (fold change) of Relish (A), Dorsal (B), Cactus (C), Vank86 (D) and Vank101 (E) are shown. Data are represented as mean ± SEM. Comparisons were performed using unpaired *t*-tests: 1 hour p.i. compared with different time points, respectively.* indicates $p < 0.05$, ** indicates $p < 0.01$, *** indicates $p < 0.001$

Unexpectedly, the same transcriptional patterns were not found, and the IκB-like protein and NF-κB/IκB both displayed time-dependent transcriptional profiles; thus, the transcription of the viral IκB-like protein may involve other transcriptional factors, which still await identification. Given that viral IκB-like genes are potentially integrated into DNA fragments in the host cell, it will be interesting to investigate the interaction between the viral promoter of the integrated DNA fragments and nuclear transcriptional factors in the host. Naturally, we believe that polydnaviruses as gene delivery systems will be useful genome editing tools in the future.

Acknowledgments The authors are grateful to Dr. Yonggyun Kim (Andong University, Korea) and Dr. Sandra Cheesman for proofreading this manuscript. The authors are grateful to Dr. Kai Zhou (University Medical Center Groningen, The Netherlands) for submitting the DNA sequences to GenBank. This work was supported in part by a grant (2013CB127600) from National Basic Research Program of China, grants from National Natural Science Foundation of China (31260448; 31060251) and a grant from Yunnan Department of Science and Technology (2013FA003) to K.L.; M.L. was supported by a grant from National Natural Science Foundation of China (31360454) and Yunnan Department of Science and Technology (2012FB120).

Compliance with ethical standards

Conflict of interest The authors declare that they have no conflict of interest.

Ethical approval This article does not contain any studies with animals performed by any of the authors.

References

1. Albrecht U, Wyler T, Pfister-Wilhelm R, Gruber A, Stettler P, Heiniger P, Kurt E, Schiimperli D, Lanzrein B (1994) Polydnavirus of the parasitic wasp *Chelonus inanitus* (Braconidae): characterization, genome organization and time point of replication. J Gen Virol 75:3353–3363
2. Anders S, Huber W (2010) Differential expression analysis for sequence count data. Genome biology 11:R106
3. Annaheim M, Lanzrein B (2007) Genome organization of the *Chelonus inanitus* polydnavirus: excision sites, spacers and abundance of proviral and excised segments. J Gen Virol 88:450–457
4. Bae S, Kim Y (2009) IkB genes encoded in *Cotesia plutellae* bracovirus suppress an antiviral response and enhance baculovirus pathogenicity against the diamondback moth, *Plutella xylostella*. J Invertebr Pathol 102:79–87
5. Beck MH, Zhang S, Bitra K, Burke GR, Strand MR (2011) The encapsidated genome of *Microplitis demolitor* bracovirus integrates into the host *Pseudoplusia includens*. J Virol 85:11685–11696
6. Beckage NE (2008) Parasitoid Polydnaviruses and Insect Immunity. In: Beckage NE (ed) Insect Immunology. Academic Press, San Diego, p 243
7. Bitra K, Suderman RJ, Strand MR (2012) Polydnavirus Ank proteins bind NF-kappaB homodimers and inhibit processing of Relish. PLoS Pathog 8:e1002722
8. Chen YF, Gao F, Ye XQ, Wei SJ, Shi M, Zheng HJ, Chen XX (2011) Deep sequencing of *Cotesia vestalis* bracovirus reveals the complexity of a polydnavirus genome. Virology 414:42–50
9. Chinchore Y, Gerber GF, Dolph PJ (2012) Alternative pathway of cell death in *Drosophila* mediated by NF-kappaB transcription factor Relish. Proc Natl Acad Sci U S A 109:E605–E612
10. Desjardins CA, Gundersen-Rindal DE, Hostetler JB, Tallon LJ, Fuester RW, Schatz MC, Pedroni MJ, Fadrosh DW, Haas BJ, Toms BS, Chen D, Nene V (2007) Structure and evolution of a proviral locus of *Glyptapanteles indiensis* bracovirus. BMC Microbiol 7:61
11. Desjardins CA, Gundersen-Rindal DE, Hostetler JB, Tallon LJ, Fadrosh DW, Fuester RW, Pedroni MJ, Haas BJ, Schatz MC, Jones KM, Crabtree J, Forberger H, Nene V (2008) Comparative genomics of mutualistic viruses of *Glyptapanteles* parasitic wasps. Genome biology 9:R183
12. Dupuy C, Gundersen-Rindal D, Cusson M (2012) Genomics and Replication of Polydnaviruses. In: NEB-M D (ed) Parasitoid viruses. Academic Press, San Diego, pp 47–61
13. Erturk-Hasdemir D, Broemer M, Leulier F, Lane WS, Paquette N, Hwang D, Kim CH, Stoven S, Meier P, Silverman N (2009) Two roles for the *Drosophila* IKK complex in the activation of Relish and the induction of antimicrobial peptide genes. Proc Natl Acad Sci USA 106:9779–9784
14. Espagne E, Dupuy C, Huguet E, Cattolico L, Provost B, Martins N, Poirie M, Periquet G, Drezen JM (2004) Genome sequence of a polydnavirus: insights into symbiotic virus evolution. Science 306:286–289
15. Flint SJ, Racaniello VR, Enquist LW, Skalka AM (2009) Principles of Virology. Molecular Biology. American Society of Microbiology, Washington, DC
16. Flores-Saaib RD, Jia S, Courey AJ (2001) Activation and repression by the C-terminal domain of dorsal. Development, pp 1869–1879
17. Hall BG (2013) Building phylogenetic trees from molecular data with MEGA. Mol Biol Evol 30:1229–1235
18. Harari-Steinberg O, Cantera R, Denti S, Bianchi E, Oron E, Segal D, Chamovitz DA (2007) COP9 signalosome subunit 5 (CSN5/Jab1) regulates the development of the *Drosophila* immune system: effects on Cactus, Dorsal and hematopoiesis. Genes Cells 12:183–195
19. Li G, Chen Q, Pang Y (1998) Studies of artificial diets for the beet armyworm, *Spodoptera exigua*. Acta Sci Circumstant/Huanjing Kexue Xuebao 4:1–5
20. Li M, Pang Z, Xiao W, Liu X, Zhang Y, Yu D, Yang M, Yang Y, Hu JS, Luo KJ (2014) A transcriptome analysis suggests apoptosis-related signaling pathways in hemocytes of *Spodoptera litura* after parasitization by *Microplitis bicoloratus*. PLoS One 9:e110967
21. Liu T, Li M, Zhang Y, Pang Z, Xiao W, Yang Y, Luo KJ (2013) A role for innexin2 and innexin3 proteins from *Spodoptera litura* in apoptosis. PLoS One 8:e70456
22. Livak KJ, Schmittgen TD (2001) Analysis of relative gene expression data using real-time quantitative PCR and the $2^{-\Delta\Delta CT}$ method. Methods 25:402–408
23. Loytynoja A, Goldman N (2010) webPRANK: a phylogeny-aware multiple sequence aligner with interactive alignment browser. BMC Bioinform 11
24. Lukashin AV, Borodovsky M (1998) GeneMark.hmm: new solutions for gene finding. Nucleic Acids Res 26:1107–1115
25. Luo KJ, Pang Y (2006) *Spodoptera litura* multicapsid nucleopolyhedrovirus inhibits *Microplitis bicoloratus* polydnavirus-induced host granulocytes apoptosis. J Insect Physiol 52:795–806
26. Luo KJ, Pang Y (2006) Disruption effect of *Microplitis bicoloratus* polydnavirus EGF-like protein, MbCRP, on actin cytoskeleton in lepidopteran insect hemocytes. Acta Biochim Biophys Sin (Shanghai) 38:577–585
27. Luo KJ, Trumble JT, Pang Y (2007) Development of *Microplitis bicoloratus* on *Spodoptera litura* and implications for biological control. BioControl 52:309–321
28. Michaely P, Tomchick DR, Machius M, Anderson RG (2002) Crystal structure of a 12 ANK repeat stack from human ankyrinR. EMBO J 21:6387–6396
29. Mitsuhashi J (1995) A continuous cell line from pupal ovaries of thecommon cutworm, *Spodoptera litura* (Lepidoptera: Noctuidae). Appl Entomol Zool 30:75–82
30. Mortazavi A, Williams BA, McCue K, Schaeffer L, Wold B (2008) Mapping and quantifying mammalian transcriptomes by RNA-Seq. Nat Methods 5:621–628

31. Park JM, Brady H, Ruocco MG, Sun H, Williams D, Lee SJ, Kato T Jr, Richards N, Chan K, Mercurio F, Karin M, Wasserman SA (2004) Targeting of TAK1 by the NF-kappa B protein Relish regulates the JNK-mediated immune response in *Drosophila*. Genes Dev 18:584–594
32. Petersen AJ, Katzenberger RJ, Wassarman DA (2013) The innate immune response transcription factor relish is necessary for neurodegeneration in a *Drosophila* model of ataxia-telangiectasia. Genetics 194:133–142
33. Saeed AI, Sharov V, White J, Li J, Liang W, Bhagabati N, Braisted J, Klapa M, Currier T, Thiagarajan M, Sturn A, Snuffin M, Rezantsev A, Popov D, Ryltsov A, Kostukovich E, Borisovsky I, Liu Z, Vinsavich A, Trush V, Quackenbush J (2003) TM4: a free, open-source system for microarray data management and analysis. BioTechniques 34:374–378
34. Simpson JT, Wong K, Jackman SD, Schein JE, Jones SJ, Birol I (2009) ABySS: a parallel assembler for short read sequence data. Genome Res 19:1117–1123
35. Stoltz D, Lapointe R, Makkay A, Cusson M (2007) Exposure of ichnovirus particles to digitonin leads to enhanced infectivity and induces fusion from without in an in vitro model system. J Gen Virol 88:2977–2984
36. Strand MR (1994) *Microplitis Demolitor* polydnavirus infects and expresses in specific morphotypes of *Pseudoplusia Includens* haemocytes. J Gen Virol 75:3007–3020
37. Strand MR, Burke GR (2012) Polydnaviruses as symbionts and gene delivery systems. PLoS Path 8. doi:10.1372/journal.ppat.1002757
38. Thoetkiattikul H, Beck MH, Strand MR (2005) Inhibitor kappaB-like proteins from a polydnavirus inhibit NF-kappaB activation and suppress the insect immune response. Proc Natl Acad Sci USA 102:11426–11431
39. Tian SP, Zhang JH, Wang CZ (2007) Cloning and characterization of two *Campoletis chlorideae* ichnovirus vankyrin genes expressed in parasitized host *Helicoverpa armigera*. J Insect Physiol 53:699–707
40. Webb BA, Strand MR, Dickey SE, Beck MH, Hilgarth RS, Barney WE, Kadash K, Kroemer JA, Lindstrom KG, Rattanadechakul W, Shelby KS, Thoetkiattikul H, Turnbull MW, Witherell RA (2006) Polydnavirus genomes reflect their dual roles as mutualists and pathogens. Virology 347:160–174
41. Yanase T, Yasunaga C, Kawarabata T (1998) Replication of *Spodoptera exigua* nucleopolyhedrovirus in permissive and non-permissive lepidopteran cell lines. Acta Virol 42:293–298
42. Zerbino DR, Birney E (2008) Velvet: algorithms for de novo short read assembly using de Bruijn graphs. Genome Res 18:821–829